Hybrid Diesel/PV Multi-Megawatt Plant Seasonal Behavioral Model to Analyze Microgrid Effectiveness: Case Study of a Mining Site Electrification

Authors:

Sani Moussa Kadri, Brayima Dakyo, Mamadou Baïlo Camara, Yézouma Coulibaly

Abstract:

Mining sites that combine energy-intensive operations with community living in areas remote from the electricity grid are increasingly developing dedicated micro-grids. Fossil oil gensets hybridization with renewable energy resources has gained momentum. Difficulties in assessing performance are experienced by operators who wish to benefit from improved performances. The designers of such systems also need additional knowledge to anticipate the solutions of the particular problems related to the power plant's implementation area characteristics. The proposed approach gives more suitable tools on the effectiveness evaluation of hybridized microgrid, combining a Heavy Fuel Oil (HFO) thermal power station with photovoltaic generator powering mine activities in the Sahelian area. The authors provide key analyses and improvement factors by seasonal behavioral modelling (SBM) of the fuel consumption of the gensets related to the overall irradiance dynamics of the PV array. Several years of data analysis results have been integrated for sharper considerations on the transient interactions impact of the PV/Diesel Hybrid Power Plant operation. The results of simulations carried out using the proposed new models, including the case of an extended system with storage unit, have been used to evaluate the levelized cost of energy, and to discuss competitiveness. This very relevant approach provides additional knowledge for designers and energetic effectiveness analysts.

processes

Hybrid Diesel/PV Multi-Megawatt Plant Seasonal Behavioral Model to Analyze Microgrid Effectiveness: Case Study of a Mining Site Electrification

Sani Moussa Kadri [1,*], **Brayima Dakyo** [2,*] , **Mamadou Baïlo Camara** [2] **and Yézouma Coulibaly** [1]

1   Renewable Energy and Energy Efficiency Laboratory, Institute 2iE, Rue de Science, Ouagadougou 01 BP 594, Burkina Faso
2   GREAH—Laboratory, University of Le Havre, Normandie 25 Rue Philippe Lebon, 76058 Le Havre, France
*   Correspondence: moussa.sani@2ie-edu.org (S.M.K.); brayima.dakyo@univ-lehavre.fr (B.D.);
    Tel.: +33-614-980-361 (B.D.)

Abstract: Mining sites that combine energy-intensive operations with community living in areas remote from the electricity grid are increasingly developing dedicated micro-grids. Fossil oil gensets hybridization with renewable energy resources has gained momentum. Difficulties in assessing performance are experienced by operators who wish to benefit from improved performances. The designers of such systems also need additional knowledge to anticipate the solutions of the particular problems related to the power plant's implementation area characteristics. The proposed approach gives more suitable tools on the effectiveness evaluation of hybridized microgrid, combining a Heavy Fuel Oil (HFO) thermal power station with photovoltaic generator powering mine activities in the Sahelian area. The authors provide key analyses and improvement factors by seasonal behavioral modelling (SBM) of the fuel consumption of the gensets related to the overall irradiance dynamics of the PV array. Several years of data analysis results have been integrated for sharper considerations on the transient interactions impact of the PV/Diesel Hybrid Power Plant operation. The results of simulations carried out using the proposed new models, including the case of an extended system with storage unit, have been used to evaluate the levelized cost of energy, and to discuss competitiveness. This very relevant approach provides additional knowledge for designers and energetic effectiveness analysts.

Keywords: behavior models; hybrid micro grid; photovoltaic/diesel plant; power transients management; performance index

1. Introduction

The African context requires new approaches to electrification systems, in particular to distributed energy production and management solutions, in order to improve the rate of access to electricity for people, particularly in rural areas, but also in the electrification of remote mining activities. These mining units are usually located outside the expandable areas of the grid, so electricity for the entire activity is provided by a thermoelectric generator using diesel engines. However, with the declining cost of renewable generation technologies such as solar and wind, the current trend is to combine solutions based on fossil fuels with renewable energies for the purpose of fuel economy and sustainability [1]. The benefit of such hybridization has been suggested in the reviewed studies [2–5]. In particular, hybrid PV/Diesel solutions are becoming increasingly attractive due to the effects of reducing supply costs coupled with fuel savings for the off-grid site [6]. Aiming for this involves modifying the approach in terms of the structural design and power management for the entire plant.

The Essakane gold mine is located in northeastern Burkina Faso (Ouest, Africa). The geographical coordinates of the mine are defined as follows: latitude 14°22′59″ N and

longitude 0°4'34″ E. Figure 1 shows the country solar resource map, provided by World Bank Group for preliminary studies.
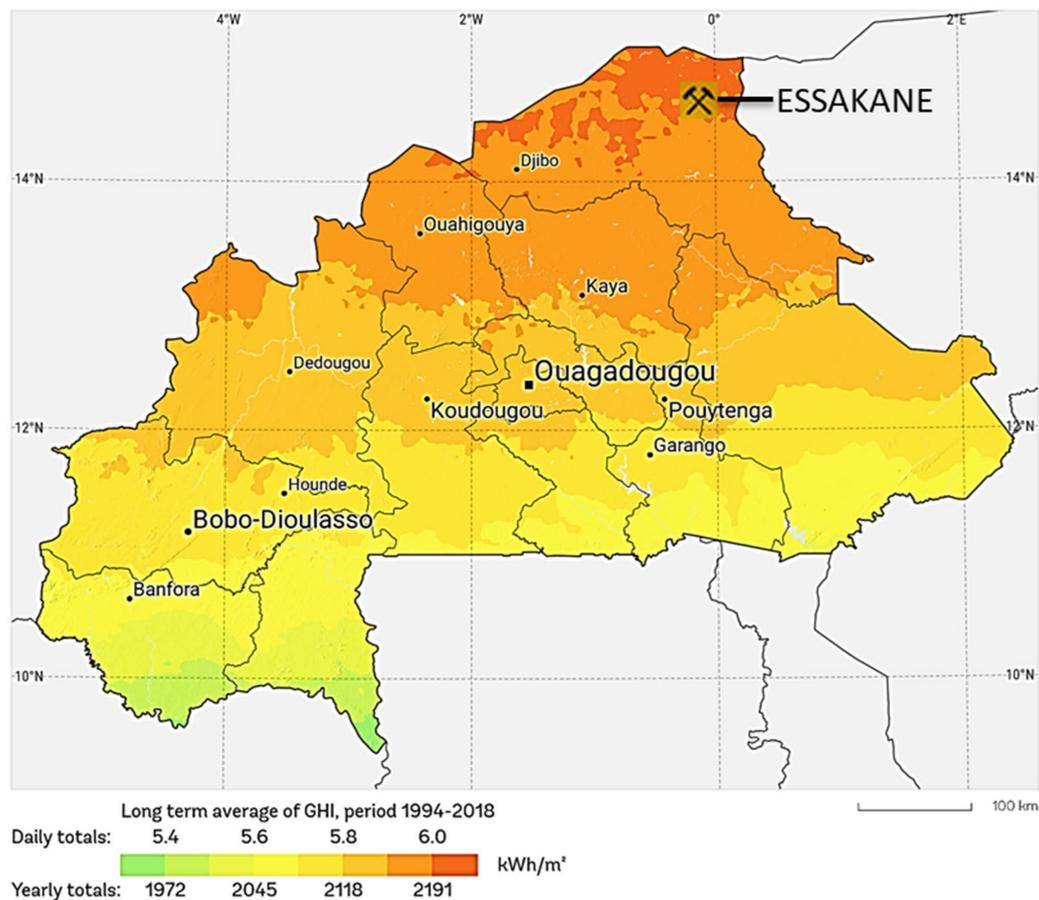

Figure 1. Country solar resource map and geographical location of the Essakane mine site.

The present study is based upon several years' of operation data analysis from the existing ESSAKANE PV/Diesel Hybrid Power Plant used as reference (Figure 2).
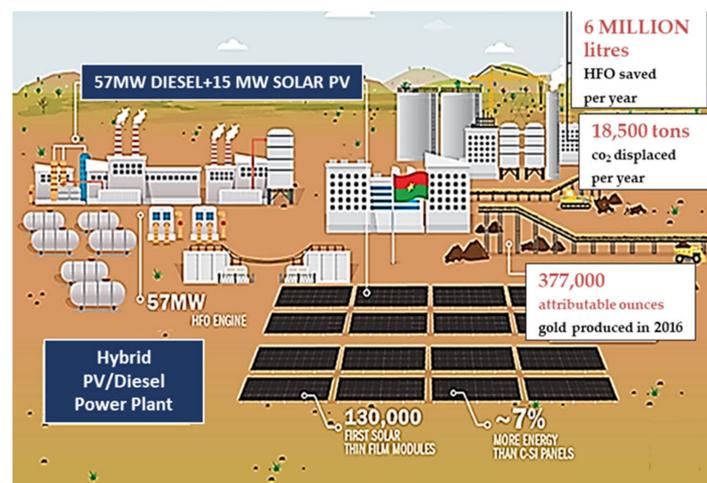

Figure 2. IAMGOLD Essakane (Burkina Faso) project (2018) flyer, PV/Diesel Hybrid Power Plant, with its key data.

This is an area not covered by Burkina's National Interconnected Grid (RNI). The mine had built an off-grid solution based on a thermal Heavy Fuel Oil (HFO) power plant that has been more recently (2018) hybridized with solar PV as a renewable power system [7]. The plant has been designed as a self-sufficient micro-grid with fuel saving targets of reducing the carbon footprint of the business, while ensuring a reliable supply and cost-effective system. In this article, a novel approach to the design and sizing of PV/Diesel hybrid power plants that are stand-alone, or integrated to a weakly meshed electricity grid, is proposed. Figure 2 gives an overview of the plant and the main goals expected for the Essakane project.

Traditionally, electricity demand in insulated sites (rural electrification, electricity needs of industrial or mining sites) is met by conventional technologies using diesel (Diesel Group) or another fossil fuel [6]. However, due to the rise in the price of such fuels and their negative impact on the environment in terms of CO_2 emissions, the trend is to hybridize conventional thermal technologies with renewable power sources as conducted with the Essakane PV/Diesel Hybrid Power Plant (Figure 3). Nevertheless, the intermittent nature of renewable reflected in the electrical power generation is considered disadvantageous [8–12].
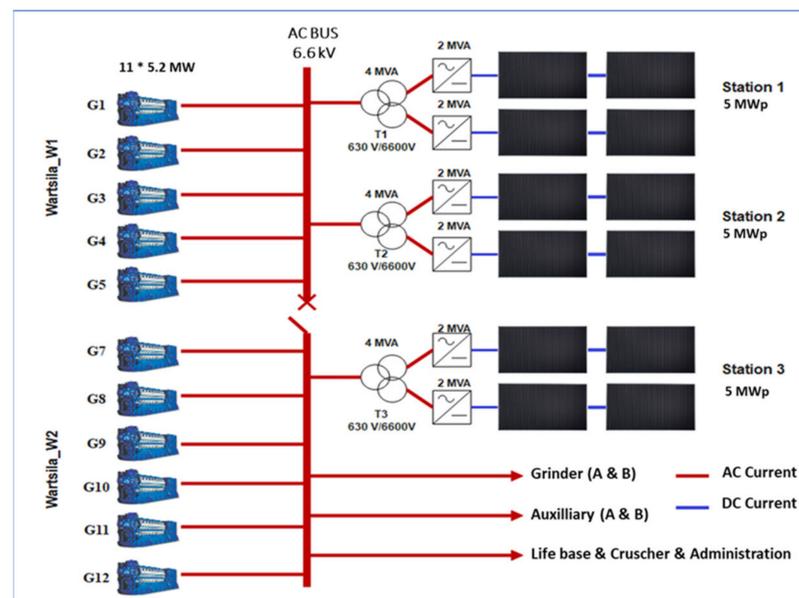

Figure 3. Structure of the Essakane PV/Diesel Hybrid Power Plant with engines and PV Array.

The interaction of several different generation sources of different natures makes the approach to hybridization quite complex. Indeed, the choice of an optimized configuration of a hybrid power generation system is affected by various factors, such as the availability of energy sources, the specificities of sites [13], as well as technical and social constraints. These factors influence cost and reliability. So, the techno-economic analysis of the hybrid system is essential for the efficient integration of renewable energy resources [14]. It must result in implementing a relevant sizing method in order to ensure the best performance and lowest investment and operating costs.

According to [13–20], hybrid system design techniques can be divided into three categories: classical, modern methods, and software tools for design and simulation. However, the predictive capacity of these algorithms is sorely reduced by the intermittent and fluctuating nature of solar energy production. Classical techniques use iterative, numerical, analytical, and probabilistic construction methods. These techniques use knowledge models mixed with behavioral ones. They are often based on deterministic assumption with simplified correlated relationships. The seasonal interaction effects on system efficiency are the gap in reviewed literature. Looking at Figure 4, it can be seen that monthly moderate variation exists and could be considered by a long-term seasonality index 1.26. It is smaller

than the European mild climate index (2.97 in France). However, in real time and in the shorter term (daily) the study shows that disturbance occurrence lead to significant changes that can be retrofitted to better size the plant with better fitted data.

(**a**)
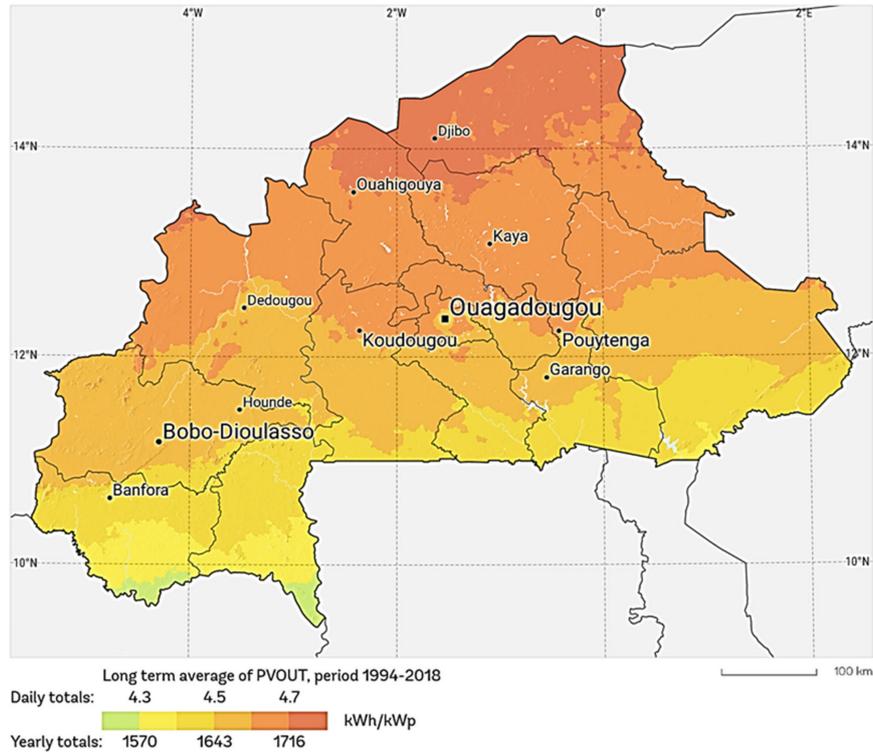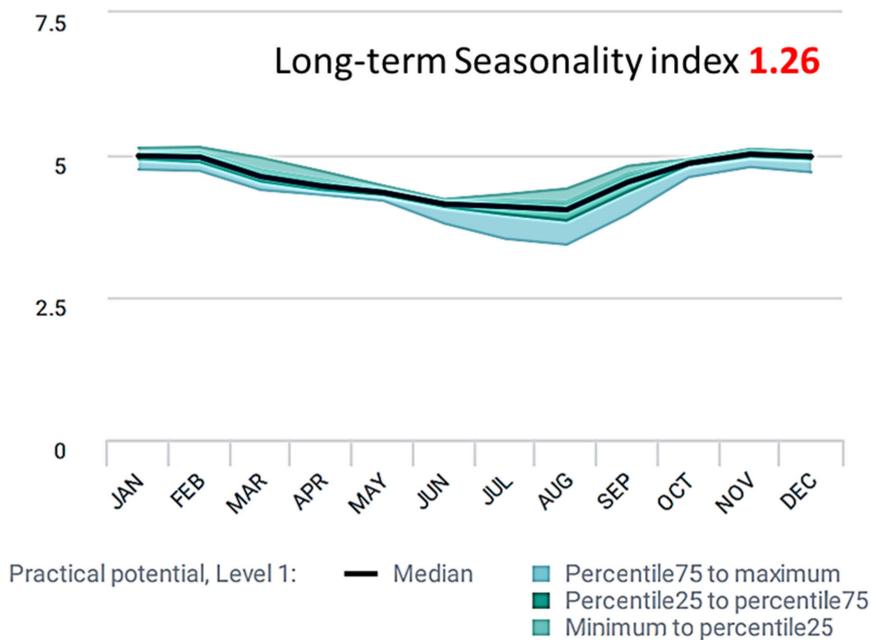
(**b**)

Figure 4. (**a**) Long-term photovoltaic power potential, and (**b**) monthly variation of output.

Using more accurate partial behavioral data is relevant and puts emphasis on the insufficiently known and considered. The factors highlighted have an impact both on overall efficiencies and on the evaluation of energy performance indicators, such as the Levelized Cost of Energy (LCOE). Thus, the present study usefully achieves computer aided design components.

2. Material and Method

In this study, insulation, electricity production, and the consumption data of the energy plant are collected over years. The production data, meteorological conditions, information from the PV generators (PVG), and the diesel engines of the Thermal Power Station (TPS), were all obtained from the plant metering. The models have been carried out from data analysis conducted with the MATLAB Simulink (Version R2015, MathWorks, Netik, MA, USA) software, when suitable. Operating data for the months of February 2019 to November 2020 have been used. For this, we have extracted moments where the TPS operates with an identical number of engines (five, six, seven, eight, and nine) with the solar PV power production. Then, we established equations linking the hourly consumption flow rate (kg/h) and the power of the thermal groups operating.

The assuming fuel oil consumption, according to ISO 15550, is derived from the fuel oil consumption on the test bed provided by the manufacturer. Accordingly, the fuel oil quality and specification of the consumption can be evaluated as well, in case of particular weather conditions. These equations show that oil consumption is hardly environmental condition dependent. One must also consider control parameter tuning effects.

The determination of specific consumption (SC) under reference conditions (ISO) from other operating conditions (test) is defined by ISO 15550, according to the calculation method described below. This method consists of performing a very complex power correction and an adjustment of the fuel PCI used, according to the following formulas:

$$Be = \frac{1000 \times \left(M - S \times \frac{MLS}{3600}\right)}{P} \times \frac{3600}{S} \quad \rightarrow \left[\frac{g}{kWh}\right] \tag{1}$$

$$Biso = \frac{\alpha}{K} \times \frac{LHV_{test}}{LHV_{iso}} \times Be - EDP \quad \rightarrow \left[\frac{g}{kWh}\right] \tag{2}$$

$$K = \left(\frac{P_x}{P_{ra}}\right)^m \times \left(\frac{T_{ra}}{T_x}\right)^n \times \left(\frac{T_{cr}}{T_{cx}}\right)^s \tag{3}$$

$$\alpha = K - 0.7 \times (1 - K) \times \left(\frac{1}{\eta_{mek}} - 1\right) \tag{4}$$

K = ratio of indicated power

α = power adjustment factor

P_x = barometric pressure during the test [hPa]
P_{ra} = standard reference barometric pressure [1000 hPa]
m = 0.7 (exponent)
T_x = air temperature during test [K]

T_{ra} = reference air temperature [298 K]

n = 12 (exponent)

T_{cr} = reference charge air coolant temperature [298 K]
T_{cx} = charge air coolant temperature during test [K]
s = 1 (exponent)
mek = mechanical efficiency

Be = fuel oil consumption on test bed [g/kWh]
Biso = fuel oil consumption according to ISO [g/kWh]
M = measure fuel quantity [kg]

S = time [s]

MLS = flow of clean leak fuel [kg/h]
P = engine power [kW]
LHV_{test} = lower heating value of the fuel during test [MJ/kg]
LHV_{iso} = lower heating value of the fuel oil ISO [MJ/kg]

EDP = Engine driven pumps [g/kWh]

In order to have reference values of the specific consumption of the thermal units, we referred to the results obtained during the tests of the on-site commissioning of the mine. Table 1 shows the test conditions and results for genset G8.

Table 1. Tests conditions and results for genset G8.

Test N°	Load [%]	Speed	Fuel	Power [kW]	Air Press [hPa]	Air Temp [°C]	Coolant Temp [°C]	Meas.fuel Amount [kg]	Mean Time [s]	Meas. consumption [kg/h]	Clean Leak Fuel [kg/h]	Eng.driven Pumps [g/kWh]	Be [g/kWh]	Biso [g/kWh]
1	100	750	HFO	5447	998.2	29	35	60	197.9	1091.5	4.320	0	199.6	190.5

Lower heating value during test [MJ/kg]: 41,120
Lower heating value (ISO) [MJ/kg]: 42,700
Mechanical efficiency (η_{mek}): 0.80

These results show a specific consumption of 199.6 g/kWh for on-site test conditions, which corresponds to a consumption of 190.5 g/kWh under ISO conditions.

The generic approach to the hybridization of electrification solutions challenges defining candidate architectures, considering multiple technical and economic criteria to make projects profitable. Fuel specific consumption is a key point for global performance evaluation.

At this point, the work undertaken aims to find behavioral models if no knowledge-models are available, in order to better analyze interaction scenarios that satisfy the electrical demand of the mining activity. The analysis is based on multi-annual seasonal operating data from the hybrid power plant at the Essakane gold mine.

2.1. Study Scope, Objectives and the Case-Study in Brief Overview

2.1.1. Objectives in Characterizing Interactions

A particular feature of hybrid power generation systems for industrial applications is the use of fossil fuel generators. According to [8,21], the hybridization of conventional thermal power plants with solar photovoltaic energy offers a promising solution to reduce production cost and environmental impact, but it also involves considerable uncertainties and risks that may compromise the availability and quality of supply. From an operational perspective, the large-scale integration of intermittent renewable sources could lead to unmet demand, electrical instabilities, and equipment damage. The performance and lifetime of conventional fossil fuel engines are likely to be altered by repeated transient operation. Control strategies and sizing methodologies must be adapted to address the high reliability constraint, while dealing with significant production uncertainties. Optimization techniques must therefore integrate these phenomena into their algorithm, while maintaining the ability to identify the most economical solution. This requires, in some cases, the adoption of specific modelling tools and the construction of new gauges.

This article proposes to characterize the transient effect of solar production on the performance of a PV/Diesel Hybrid Power Plant. This plant consists of 11 thermal units with a total capacity of 57 MW and a solar power plant of 15 MWP peak power. As shown in Figure 2, the hybridization of the plant should save 6 million liters of fuel per year and reduce CO_2 emissions.

In order to formalize the interactions between the different sources and the load, the operation of the thermal generators and their control mode were analyzed. The interactions at the Point of Common Coupling (PCC) with the photovoltaic generators have then been characterized. Assuming that the permanent control of the maximum power point tracking is carried out, the induced disturbances have been highlighted and correlated to the seasonal evolution of the sunshine of the site. A more adequate characterization of the solar resource was carried out. Based on observations, we have built and proposed the consumption patterns of the thermal power plant in relation to the quality of the interactions at the PCC. In doing so, two consumption patterns of the interacting thermal power plant were clearly identified.

2.1.2. Approach to Power Analysis

The proposed approach suggests that dynamic reaction balancing the common coupling can negatively affect fuel consumption when numerous high transients occur. This can be both due to the fluctuations from the demand side and/or from the complementary power production. The peak power penetration rate of solar PV is planned at 26%. This ratio is defined as the standard test condition peak power of PV generator versus the total installed power of gensets. It can be used for acquisition cost comparison, but not for operation.

The activities of the mine consist mainly in the extraction and processing of ores for the production of gold. Thus, the main areas of electricity consumption related to the activities of the mine are presented in Table 2. The mine plant operates 24 h a day, has 04 grinders with a unity power of 7 MW, and its auxiliaries represent 90% of the total power demand.

Table 2. Consumption areas of the mine.

Zones of Mine Consumption	Devices/Needs
Factory (Mine)	Tranche A: 2 × 7 MW grinder Auxiliaries Unit A of the factory Tranche B: 2 × 7 MW grinder Auxiliaries Unit B of the factory
Career Administrative Life Base Camp	Crusher Business administration Facilities and safety safe working environment

The analysis on the number of occurrences of the electrical power demand (Figure 5) over an observation period, from March to June 2019, shows that the average power demand remains near 40 MW.

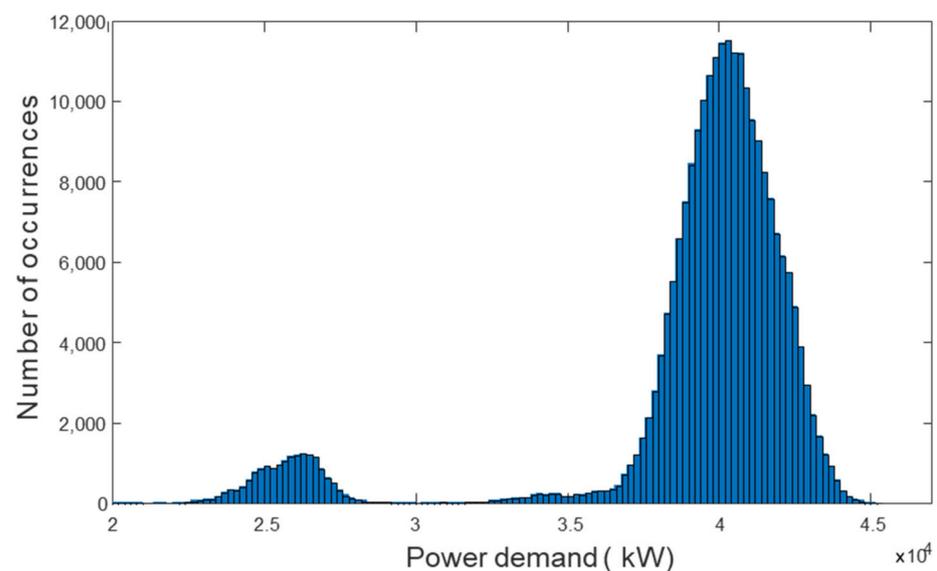**Figure 5.** Number of point occurrences in power demand data from March to June 2019.

As an example, the time-based load profile of the entire activity of the mine for the month of March 2019, is shown in Figure 6. It can be seen that the load profile evolves close to an average value of 40 MW with some variations correlated to the shutdown and start-up of the grinders of the mine's A and B tranches.
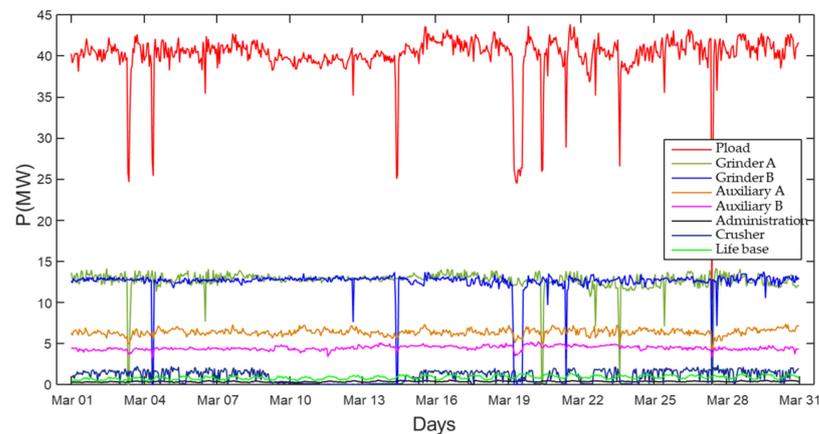
Figure 6. Mine load profile for the month of March 2019.

Since we have to produce electricity for the whole site, we will consider the electrical load profile as the service to be rendered (SR). It is variable according to the power demand P_{SR} of the electrical equipment:

1. Two entities contribute in a strictly complementary manner and in "real time" to the production of electricity. These are the thermal generators on one hand, and the PV generators on the other. A busbar and three transformers allow to create the right coupling conditions. The load profile does not change much at full power, it is modified at low frequency, and changes little around 40 MW (Figure 6);
2. The TPS are controlled in a classical way by operating under loop, which synchronizes and ensures the secured and balanced dispatching;
3. The PVGs operate under the control of an algorithm (MPPT) imposing in real time an injection of power in connection with the variations of the sunshine;
4. The interactions are then under the influence of the load profile, the variations of the sunshine, and the operational multi-criteria control rules. At the PCC, we observe an exact compensation effect between the generated (TPS and PVGs) and totalized (P_{SR}) power at the busbar levels:

$$P_{SR}(t) = P_G(t) + PV_G(t) \;\rightarrow\; \int P_{SR}(t) = \int P_G(t) + \int PV_G(t) \tag{5}$$

The share of PV on the service rendered SR for a given period T is written:

$$E_{PV} = \int_0^T PV_G(t) \; et \; E_G = \int_0^T P_{SR}(t) - \int_0^T PV_G(t) \tag{6}$$

$$E_{SR} = E_G + E_{PV} \tag{7}$$

5. The reactive power exchanges are assumed to be well managed by means of generator excitation, the inverters control, system inductors, and capacitors. Only active power balancing is considered in the management policies that are later exposed.

2.2. Seasonal Sensitive Monitoring of the System

2.2.1. Average Monthly Irradiation on Site

The instantaneous measurements of irradiance G (W/m^2) collected at the mine site were used to determine the average daily irradiance H ($kWh/m^2/day$) for the different months of the year 2020. It can be seen in Figure 7 that the irradiance value varies from 6.965 $kWh/m^2/day$ for the month of February to 5.428 $kWh/m^2/day$ for the month of August (i.e., LTSI close to 1.28). The annual average is estimated at 6.149 $kWh/m^2/day$. In this Sahelian area, there is a rainy season and a slightly longer dry one. It can be seen that

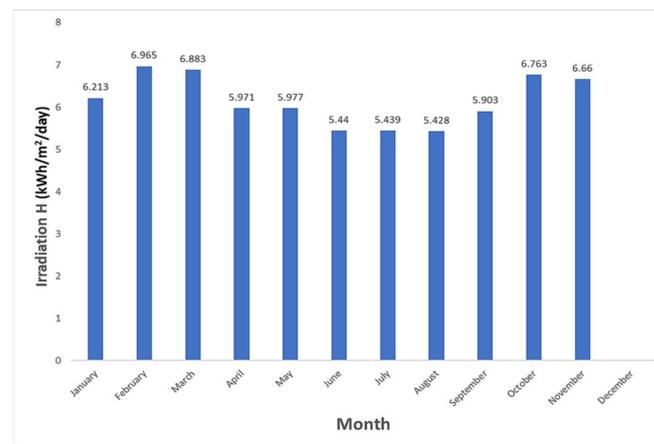the lowest value of average irradiance occurs in rainy season particularly in August, the cloudiest month.

Figure 7. Monthly average of daily irradiation on site for the year 2020.

2.2.2. Categorization of Seasonality of the Solar Irradiance

To make this analysis, the satellite data of the daily horizontal global irradiation in kWh/m^2/day for the mine site have been retrieved from a NASA database (www.power.larc.nasa.gov) accessed on 1 March 2021, for the years 2019 and 2020. Taking these data as a collection of information, the plot of Figure 8 highlights two typical periods in terms of variability of daily irradiation. (Figure 8):
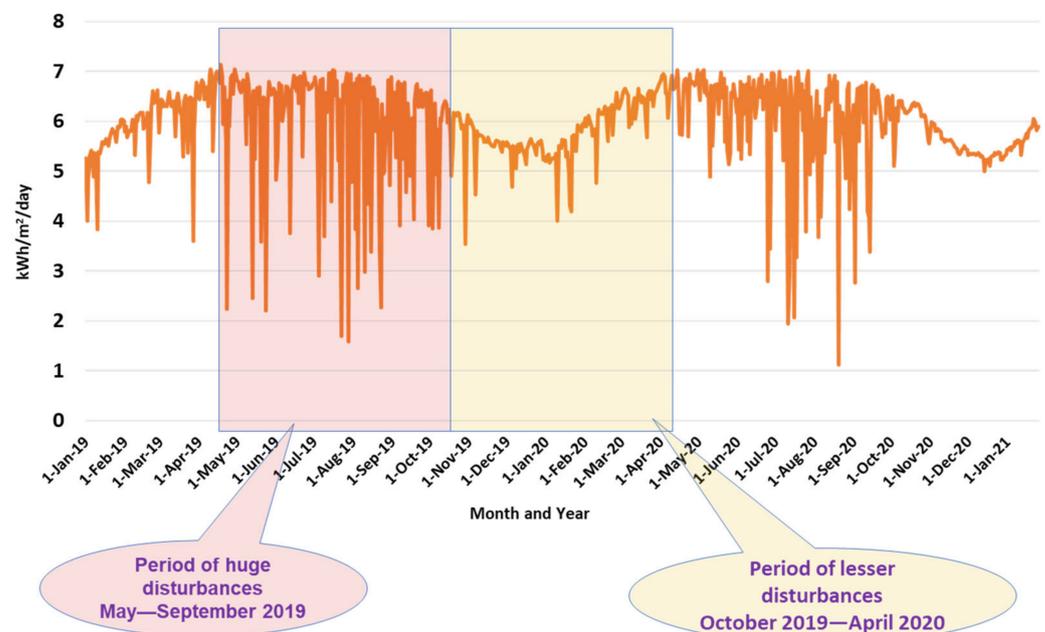
Figure 8. Solar radiation on the Essakane site from 2019 to 2020.

A period of frequent huge disturbances: this is the period from May to September, which corresponds roughly to the rainy season of the mine site.

A period of less disturbance: this is the period from October to April and corresponds to the dry season of the mine site.

It is then necessary to understand and characterize the specific behavior of the power plant undergoing the energy impact of these dynamic fluctuations during the two seasons.

It can be introduced in a short-term seasonality index defined likely LTSI, but evaluated in day time (between 1 and 2.8).

The interactions induced by such dynamic behavior needs to be characterized. It is known that the diesel engine reacts badly to too frequent changes in power rate in terms of fuel consumption and servicing.

This section deals with how to consider the variability of the irradiation during the year and of the irradiance over a short- and medium-term observation window.

2.3. State of the Art of Production System Technologies and Operating Principles of Season Sensitive Autonomous PV/Diesel Power Plants

2.3.1. Generator Set Technologies

Generator set technologies consist of autonomous devices capable of powering electricity by constant speed (i.e., fixed frequency) internal combustion engines energized from HFO. Their use is widespread in developing countries due to the unavailability or unreliability of the network [22]. They are commonly used as the main source or backup of electrical power source for mining industries. The main features and advantages of generator set technologies are [23]:

- Low investment costs—due to their widespread application and manufacturing.
- High reliability—diesel engines are proven and robust machines, well suited to harsh operating environments. Engine maintenance is based on the amount of regular operating hours and is therefore quite predictable in such context.
- Fast start and loading requiring minimal warm-up time before they can accept the load.
- Good load fluctuations tracking capabilities.
- Diesel engines are relatively easy to install.

The constant-speed generator technologies are widely used today but the advanced power electronic interface allows for increasingly taking advantage of the variable-speed generator set. As shown in Figure 9, the proper way to provide variable power is to operate at variable speed in contradiction to the need to generate electrical power at a fixed frequency. The use of such advanced technologies capable of this functionality is irrelevant here.
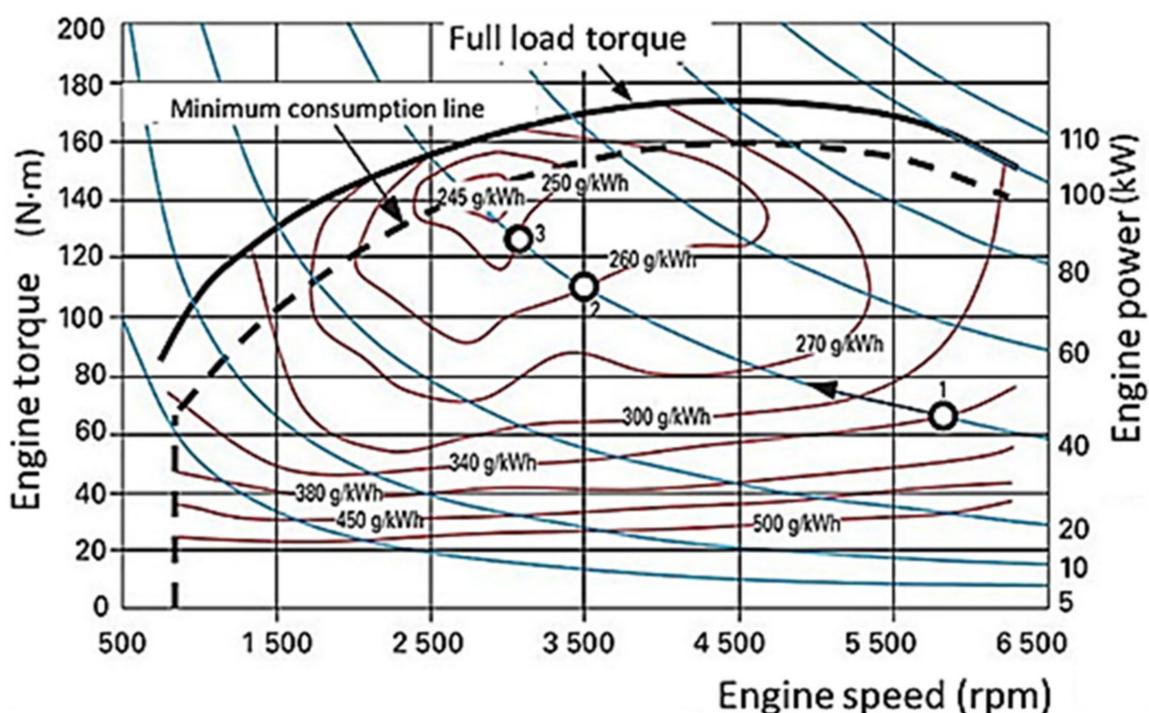

Figure 9. Map of complex specific consumption (red curves) and output power (blue curves) of a diesel engine versus rotation speed.

- Fixed speed generator sets

The engine drives a synchronous generator that converts the mechanical energy into electricity.

The efficiency that depends on the load is maximum at the rated power delivery point. According to the author [24], the (thermoelectric) efficiency of the units is between 25% and 38%, Figure 10, close to the rated power P_N (typically, between 70 and 100% of P_N). For operation below 40% P_N a decrease of efficiency and a surge in the corresponding specific consumption generally occur. Therefore, it is not cost effective for fixed speed gensets to operate below a minimum load. The fuel consumption of a generator set during operation is defined either by its hourly consumption in [kg/h] or [L/h], or its specific consumption in relation to the electrical energy delivery in [g/kWh] or [L/kWh].
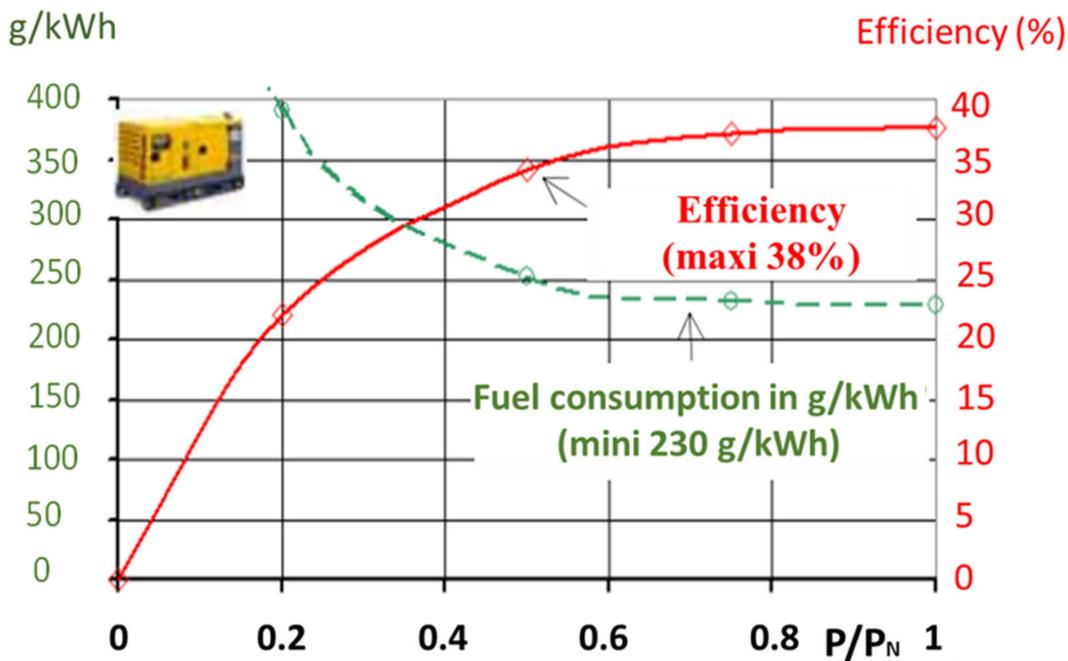

Figure 10. Characteristics (efficiency and consumption as a function of the load rate) of a diesel generator [24].

According to [23,24], the hourly consumption characteristic of a generator can be considered as a quasi-linear function of the power output. This means that the higher the power output, the higher the hourly fuel consumption. On the other hand, the specific energy consumption is generally non-linear to the output power and increases exponentially at low load. The hourly consumption function over full range running can be approximate by second-order polynomial under governor control [25,26].

$$HC_{lu}(P_u(t)) \cong \alpha \times P_u^2(t) + \beta \times P_u(t) + \gamma \tag{8}$$

HC_{lu} the rate of fuel consumed by the generator (L/h);
P_u the output power of the generator (W);
α, β, γ, provided by the manufacturer from the data sheets.

In the case of running regime over 40% power ratio a linear approximation of hourly consumed rate of fuel is very relevant. According to [24], the hourly consumption HC (in kg/h) of a generator set operating at constant speed can be modeled by an affine law of the form:

$$HC_{ku}\left(\frac{P_u(t)}{P_N}\right) \cong K \times \frac{P_u(t)}{P_N} + HC_{ku0} \tag{9}$$

K (fuel curve slope) and HC_{ku0} (generator intercept coefficient) are parameters tuned from consumption curve for a given generator set; PN represents the rated power of the generator set; Pu(t) represents the instantaneous output power. This formula is Homer-pro software user-friendly and easily integrates it's the design process.

To vary the power during transients, it is necessary to play on the Mean Effective Pressure (MEP), the number of thermodynamic cycles being given. Increasing the MEP is performed by inflating the real cycle, therefore by allowing in the cylinder a mass M (Kg) of fuel mixture as high as possible. Dynamically, due to the need to enrich the mixture to obtain the maximum torque of the engine, the quantity of unburned matter increases, therefore the combustion efficiency is less good. Thus, as will be established, the average power is delivered with a greater efficiency penalty the greater the transient variations involved. This complex internal combustion phenomenon has led to the development of a behavioral model that globalizes the impacts in terms of energy efficiency. The interaction of such thermal generator at the PCC with PV solar power injection suggested the definition behavioral model related to "Quasi-static Solar Profile (QSP)" (disturbances free case) and "Dynamic Solar Profile (DSP)" (huge disturbances case).

2.3.2. Photovoltaic System and Power Production Modelling

A photovoltaic production chain (Figure 11) [27–32] consists of a cascaded photovoltaic generator, converter, and transformer. Usually, the converters integrate a control system called MPPT (Maximum Power Point Tracker), which allows to recover the maximum power available from the PV generator. A filter is added after the inverter to reduce the Total Harmonic Distortion rate fed into the grid. A step-up transformer is often used as an interface between the inverter and the grid in order to adapt the output voltage of the grid and it ensures galvanic insulation for security purpose.
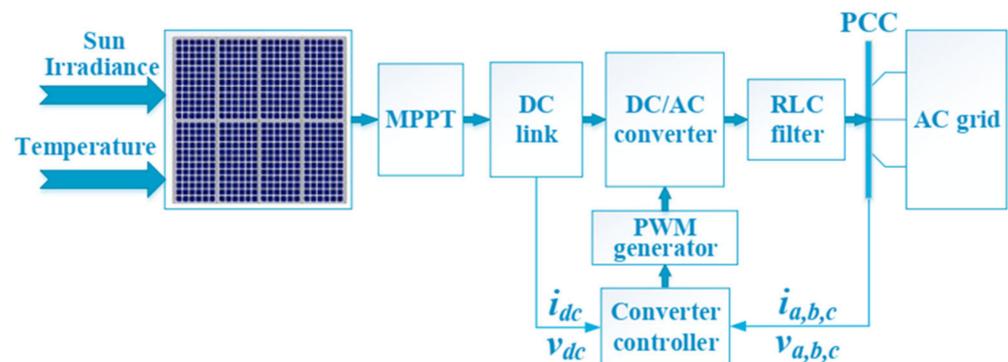
Figure 11. Example of a photovoltaic power generator path (transformer free) [27].

The photovoltaic generator consists of several modules in matrix association (series/parallel); modular blocs are constituted considering space, maintainability, and power management constraints. Depending on the technology of the cells, assuming relevant MPPT running, the instantaneous power model of a photovoltaic generator [30,31] can be expressed by the equation:

$$P_{PV}(t) = P_{PV_{STC}} \times \left(\frac{G(t)}{G_{STC}} \right) \times \left[1 - \delta \times \left(T_{module}(t) - T_{module_{STC}}(t) \right) \right] \tag{10}$$

where

$P_{PV}(t)$: Instantaneous power produced by the modular PV field in Watt;
$P_{PV_{STC}}$: Peak power of the modular PV field under Standard Test Conditions (STC);
$G(t)$: Global solar radiation received in the plane of the modular PV field in W/m²;
G_{STC}: Solar radiation under STC conditions in W/m²;
δ: Module temperature coefficient in %W/°C;
$T_{module}(t)$: PV module temperature in °C;

$T_{module_{STC}}$: Temperature of PV modules under STC conditions in °C.

Solar power conditioning evolves under the control of maximum power tracking automate. So, the behavioral model, including power path efficiency, is given in Figure 12. The output delivers AC active power to the PCC.
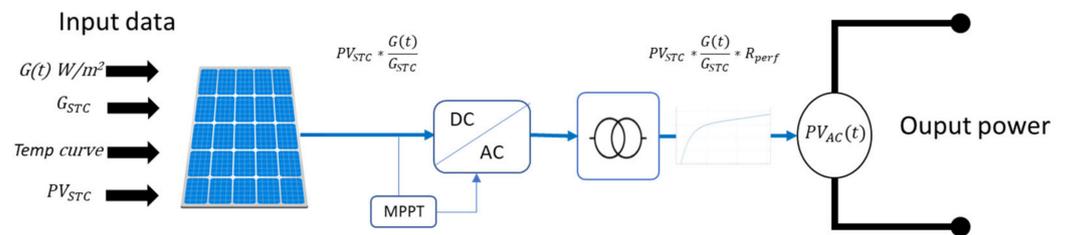

Figure 12. Behavioral model of PV$_G$.

2.3.3. Structure and Operating Strategies of the Essakane PV/Diesel Hybrid Power Plant

The complete PV/Diesel Hybrid Plant consists of a thermal power plant coupled with the solar PV plant, as shown in Figure 13. The thermal power plant includes 11 thermal units of the same characteristics of the Wartsila brand, with a unit rated power of 5.2 MW. The array of six string solar power panels is structured in two sections with 10 MWp and 5 MWp peak STC power. The power conditioning and link to the PCC are obtained with cascaded inverters and three coil transformers. These components number and rated values are as followed:

- 132,000 PV panels: 96,000 panels of 115 Wp and 36,000 panels of 117.5 Wp $(3 \times (32,000 + 12,000))$;
- 06 ABB trade mark inverters of 2 MVA rated power;
- 03 ABB trade mark transformers of 4 MVA rated power.

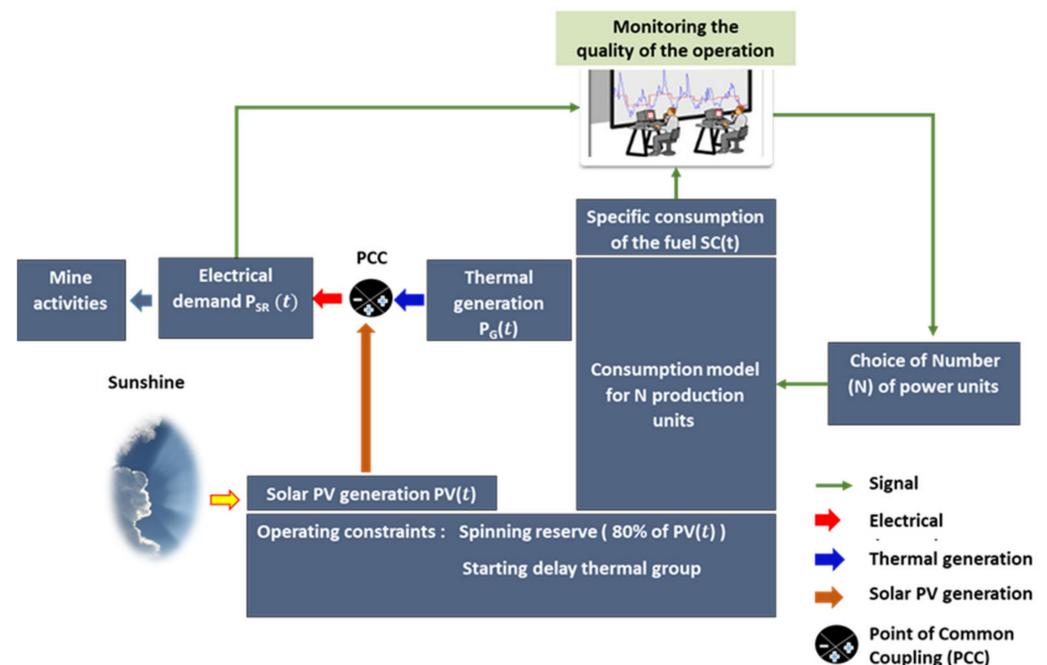**Figure 13.** Functional diagram of the operation of the Essakane Hybrid Power Plant.

According to the reconstituted process management diagram (Figure 13), the instantaneous contributions of solar PV production and thermal production makes it possible to satisfy the electrical power requirement of the mine's activities. In doing so, the operation of the hybrid power plant is based on three principles, which are:

- To regulate the integration of the solar PV power acting as unpredictable "negative load" by providing real time compensation of fluctuations;
- To maximize the efficiency of the hybrid system through operator dispatching rules, keeping both thermal generators and PV always close to the best running point with the active MPPT;
- To guarantee the stability of the hybrid system by means of a spinning reserve and/or the limitation of the active power of the solar PV plant. The spinning reserve is sized to recover the energy surge during hazards like sudden power decrease/increase by cloud shadowing or load and even technical events.

The cumulative flowmeter data collection correspondence to the fuel oil consumption meters was verified to prove reliability and accuracy. In the same way, electric energy delivered was computed. The errors (Table 3) found are respectively close to 0.2% and 0.04%.

Table 3. Summary of G12 test results.

Day 8 November 2019	Electricity Production in kWh	Fuel Oil Consumption in kg
Obtained with sampled data collection from 7:00 a.m. to 5:00 p.m.	41,812	9106
Values on the Meters from 7:00 a.m. to 5:00 p.m.	41,792	9126
Deviation	0.04%	0.2%

Data collection for the study took place from February 2019 to November 2020. The data collected were then structured and classified. Multiple levels of data analysis time horizons were created to reflect and focus the main changing weather phenomena (dry and rainy seasons). The data collected were time-stamped and were identical to the acquisition time step. The time step of the collected data varies from 1 s to 44 s and refer to Greenwich Mean Time (GMT).

2.4. Analysis Patterns of Behavior

2.4.1. Methodology

In order to propose relevant behavior models and some novel metrics, a combined system analysis have been adopted (Figure 14) based on the actual Essakane PV/Diesel Hybrid Plant. This approach consists of setting up a virtual system that serves as a decision-making support tool based on relevancy (measured data adjustment with simulation provided ones) and abstraction (modeling adjustment with digital architecture capability). Six key points focused are described below:

- Measurement and data collection: It is necessary to inventory the instrumentation of the existing system and to complete it if necessary, in accordance with the necessary data and data processing to successfully characterize the behavior of the system;
- Analysis of interactions inside the system: This step consists of analyzing the operation mode of the PV/Diesel hybrid system by focusing on the interactions at the common coupling point. It will identify operating constraints and the energy exchange balance and adequacy;
- Behavioral model: Several behavioral models will be developed, including the consumption model of the thermal power plant, the behavioral model of the solar PV plant at the point of coupling, and the behavioral model of the genset losses. The development of these models consists of establishing correlations between data formal relationships between the inputs and outputs of the subsystems;
- Knowledge Model: This is about establishing definitions of causalities that make the outputs of the subsystems predictable from the inputs, the physical parameters are clearly expressed in such cases;

- The development of operating scenarios and simulations: this involves proposing operating scenarios that are not currently feasible on the physical reference system. These scenarios are developed to characterize special operations that are not feasible in practice due to potential damage or time lack.
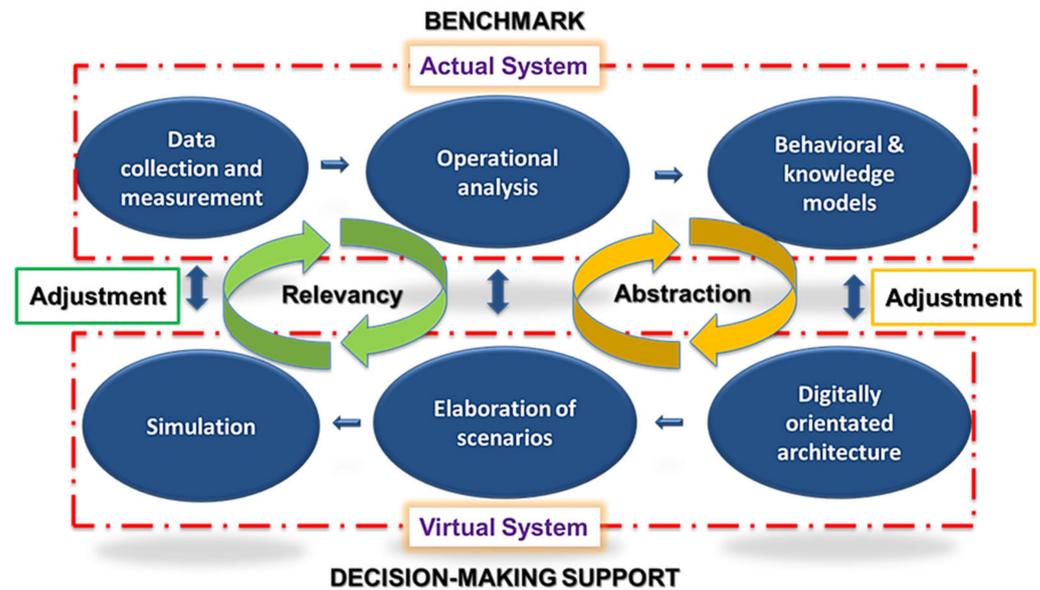

Figure 14. Graph of general approach to data analysis and system modelling.

2.4.2. Behavioral Models of Thermal Plant Consumption
Observation of Interaction between Solar and Thermal Production at the Coupling Point

In order to analyze the interaction phenomena between solar production and thermal production, the operating data of the hybrid power plant for the month of March 2019 have been here considered. According to the control diagram of the plant (Figure 10), the instantaneous thermal and solar PV complementarily power the mine's electrical demand. As shown in Figure 15, several interaction phenomena can be noticed at the PCC measurements. Thus, we can observe:

- The behavior gives evidence to the instantaneous complementarity of the solar and thermal powering mine activities;
- Daily magnitude variation of solar PV production appears. Some days, although few, show superposed disturbances.

The behavioral modelling is carried out on the basis of the operating data for the months from September 2019 to February 2020, mixing dry and rainy seasons. For this purpose, we extracted all the instances where the thermal power plant operates with an identical number of groups (five, six, seven, eight, and nine) in the presence of the solar PV production. Then, we established equations linking the hourly consumption rate (kg/h) and the power of the thermal units in operation.

The plant operates with a variable number of active thermo electrical generating units (N varying 1 to 11). According to the driving process in Figure 15, the plant manager sets the number of units in operation with regard to the specific consumption level of the thermal power plants, added with other safety conditions such as spinning reserve. Therefore, the proposed approach assumes that the behavior of the thermal power plant in terms of fuel consumption depends strongly on the number of units (groups) in operation, and also on the so called quasi-static or dynamic interaction regime, as sunshine varies. These phenomena are season dependent. In order to demonstrate the changes in the performance of the thermal power plant, attributable to the sunshine regime, a consumption analysis

according to the classification "Quasi-static Solar Profile (QSP)" and "Dynamic Solar Profile (DSP)" has been carried out.
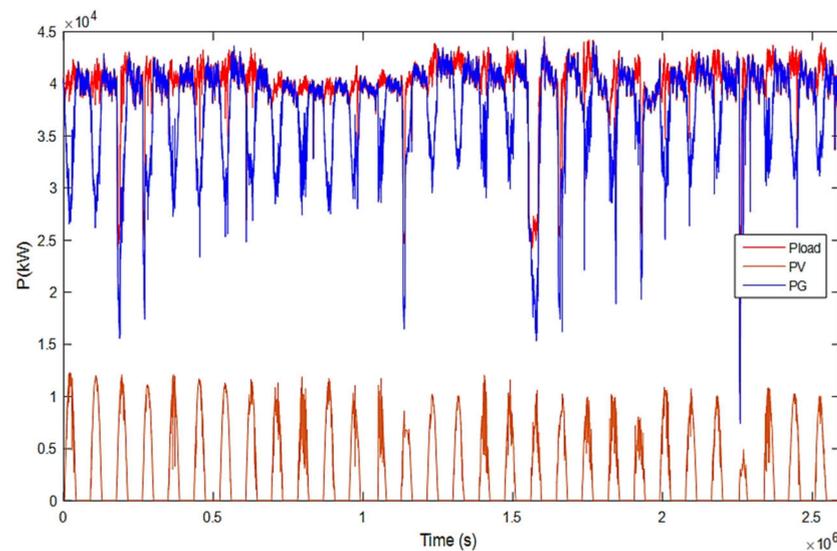
Figure 15. Interaction phenomena between solar production and thermal production and electricity demand.

Developing Models in Quasi-Static Solar Profile (QSP) or Dynamic Solar Profile (DSP) Conditions

The research for the QSP or DSP behavior model is performed by merging, with consistency, the quantitative information (generators of the same type and identical metrology). In doing so, a Unit Referenced Model (URM) under QSP/DSP type is constructed, according to the method shown in Figure 16. This specific model makes it possible to extrapolate the QSP kind consumption behavior of the plant, according to the number of gensets in operation.
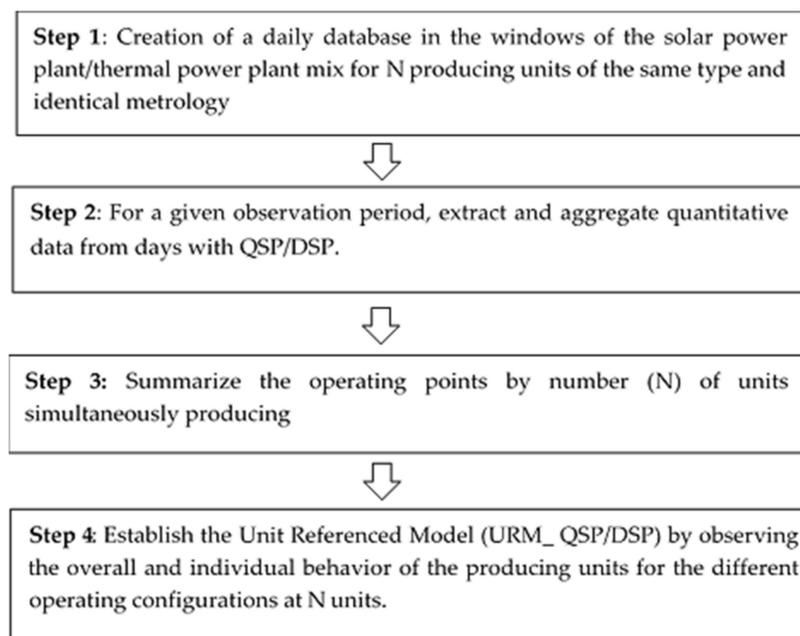
Figure 16. Method of developing URM_QSP/DSP consumption models.

This method of searching a unit reference model QSP/DSP was applied to a chosen seasonal period (example of September 2019 to February 2020). Two sets of data corresponding to 20 days of each type (Figure 17) were extracted from measurements on five production units (G7, G8, G10, G11 and G12).

(a)

(b)
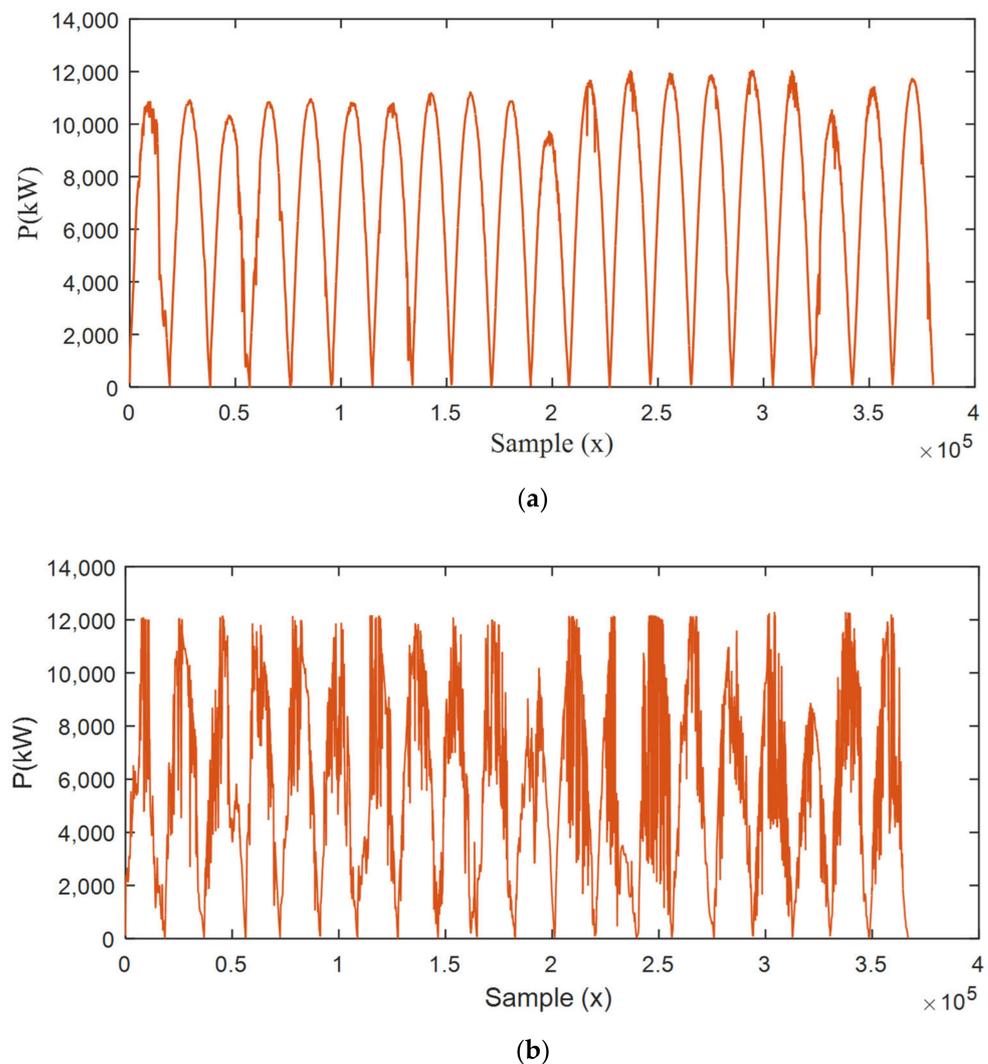
Figure 17. Two sets of data corresponding to 20 days under QSP/DSP conditions: (**a**) aggregation of 20 QSP-type PV productions per day, from September 2019 to January 2020; (**b**) aggregation of 20 DSP-type PV productions per day, from September 2019 to January 2020.

The summary of operating points by configuration at N simultaneously producing units is given in Table 4. For each configuration a global and individual behavior model of the producing units was performed. Linear regression method was suggested by tendency curve observed.

An analysis of the overall and individual fuel consumption behavior of the generating units for different configurations confirm that:

- The producing units reveal a linear behavior for the evolution of their hourly flow according to the electrical power produced, in the form of an affine law used as Unit Referenced Model (URM) under QSP/DSP:

$$D\_G_u = A \times P_{Gu} + B_u \qquad (11)$$

- With D_Gu: hourly flow in kg/h per producing unit "u" and P_{Gu} = electrical power supplied per producing unit;
- In each configuration the overall behavior (of N unities producing) of consumption is also linear in the affine form:

$$D\_G_{Nu} = N \times D\_G_{ue} = N \times (A \times P_{Gue} + B_{ue}) \tag{12}$$

- With D_G_{Nu}: global hourly flow of N units. The index "ue" refers to an equivalent producing unit theoretically uniformized;
- The producing units have quite similar behaviors even if some disparities are noticed due, partially, to the adjustments, which are not rigorously identical for all servo loops and the inherent non linearities. A maximum error of 1.3% was evaluated between these different coefficients;
- The "A" is a multiplier or factor that reflect dynamic property of the consumption models of a unit and is roughly equal to the slope coefficient of the overall behavior model when N units producing power $P_{GNu} = N \times P_{Gue}$ is considered;
- On the other hand, the constant B_{Nu} of the global behavior model represents the sum of the constants of the "original step up" of the N equivalent producing units;
- $(B_{Nu} = N \times B_{ue})$.

Thus, the overall consumption behavior in QSP mode of five units simultaneously producing is shown in Figure 18a, and in DSP mode is shown in Figure 18b. The resulting models are represented with Figure 18c. Table 4 summarizes the total operating points analyzed per number of units operating and the prevalence rate of occurrences in the collected data during 212 h.

Table 4. Number and percentage of occurrence of operating points and corresponding total time.

Number of Units Simultaneously Producing (N)	Number of Operating Points Identified	Percentage of Occurrences in Time (%)	Corresponding Operating Time (h)
6	35,896	9.45	19.942
5	135,461	35.65	75.256
4	125,648	33.06	69.804
3	40,797	10.74	22.665
2	42,231	11.11	23.462
Total	380,033	100.00	211.129

Thus, in the light of these observations, the linear relationship between the flow rate and the electrical power generated by the overall consumption behavior can be put in the following form:

$$D\_G_N = N \times P_n \times \left(0.1888 \times \left(\frac{P_{GNu}}{N \times P_n} \right) + \frac{112}{P_n} \right) \tag{13}$$

$$D\_G_N = N \times P_n \times \left(0.187 \times \left(\frac{P_{GNu}}{N \times P_n} \right) + \frac{135}{P_n} \right) \tag{14}$$

This specific model makes it possible to extrapolate the QSP/DSP consumption model of the thermal power plant according to the number of gensets in operation.
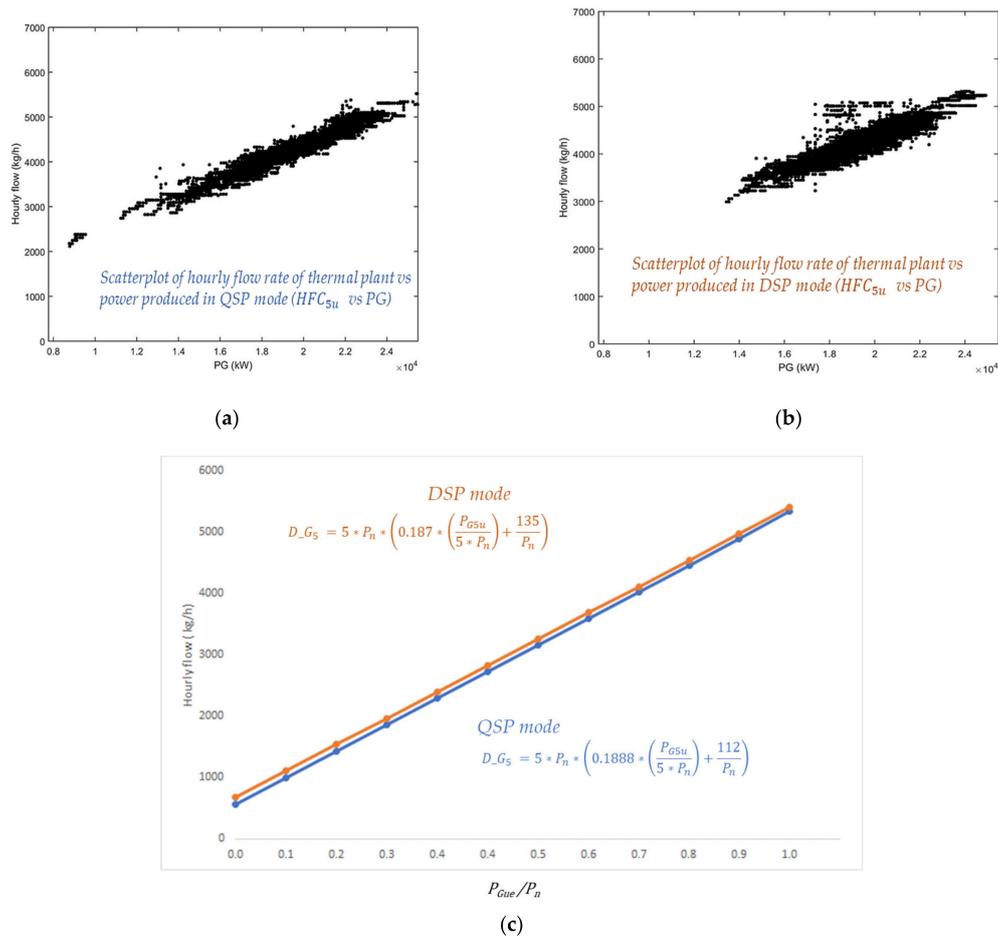
(a)

(b)

(c)

Figure 18. Behavioral models (**c**) extracted from hourly fuel flow rate measurements in QSP (**a**); and DSP (**b**); modes (**c**) behavioral models extracted from thermal plant consumption flow rate.

2.5. Evaluation of Relevancies of the Models

It is possible to assess the relevance of the models obtained according to typical post-processing scenarios. For a day such as 11 October 2019, comparisons between estimates and consumption measures provoke remarks. Over the entire day, it would be advisable to distinguish the succession of two behaviors (Figure 19). From sunrise to sunset the sunshine was disturbed (cloudy passage) therefore a DSP model was used; after sunset and before sunrise, obviously, a QSP condition had been used. The two well fitted models of behavior were applied, to respect DSP and QSP causalities. The result from behavioral models matched the meter one with 0.4% error. This evaluation (Table 5), and numerous others, demonstrated good relevancy of built behavioral models.

Table 5. Summary of fuel consumption mixed scenario QSP and DSP (Day: 11 October 2019).

| Day: 11 October 2019 with Static Load Profile and Dynamic PV Profile	Deviation [%]	Fuel Consumption in [kg]	Measurement Periods
Value in the counter index (daily report)	0	192,593	From 11 October 2019 at 6:00 a.m. to 12 October 2019 at 6:00 a.m.
Values calculated by flowmeter indicators	3%	186,680	From 11 October 2019 at 6:00 a.m. to 12 October 2019 at 6:00 a.m.
Estimated consumption Unified models QSP and DSP	0.4%	191,730	From 11 October 2019 at 6:00 a.m. to 12 October 2019 at 6:00 a.m.
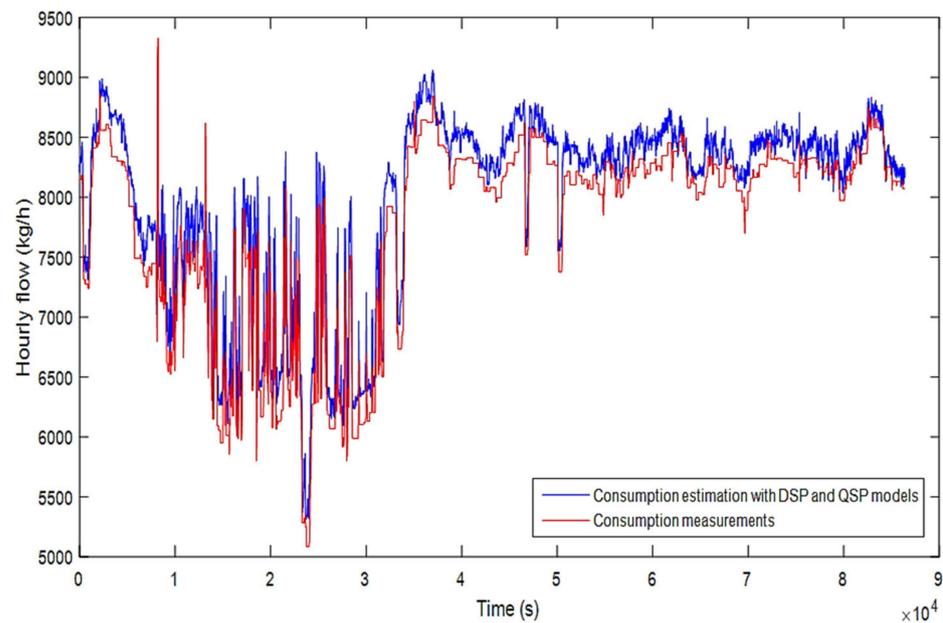
Figure 19. DSP and QSP day, evolution of measured and estimated consumption.

3. Results

3.1. Impact of Transient Regimes Due to Rapid Variation in Sunshine

3.1.1. Analysis of Fuel Consumption Patterns

The development of the consumption models of the hybrid power plant showed the impact on fuel consumption, according to the regime of interaction of the sources at the point of coupling. The parametric analysis of these consumption model's Equations (13) and (14) shows that the slope coefficients are slightly the same but the original step-up coefficient acts as a penalty and performance degradation factor in the presence of disturbances. It is therefore obvious that this phenomenon could be weighted by the intensity, frequency, and duration of disturbances. At this phase of the work, a global consideration by a simple aggregation of the effects of the disturbed periods observed in the multi-year data bank is assumed sufficient. The main qualitative interpretation is that a kilowatt of electricity produced under QSP conditions requires less fuel than the same kilowatt produced under DSP conditions. If extrapolated, it was estimated an average waste of 20 extra kilograms per generator and for one kilowatt of electricity produced under DSP conditions. This overconsumption reflects a cumulative effect of the disturbances. It should be noted that the proposed approach made it possible to estimate a potential fuel gain in the management of power production if the impact of fluctuations in sunshine could be counteracted.

3.1.2. Assessment of a Loss of Fuel Economy Due to Transient Regimes from Solar

In order to estimate a shortfall (EFG) in power delivery, we use the two consumption models adequately depending on disturbed sunshine or not, as shown in Figure 8.

- The direct mode makes it possible to calculate the consumption from the QSP and the DSP adequate models, resulting in an effective amount of fuel consumed (EFC);
- Then, we apply the average model of sunshine that leads to the same amount of energy of PVG origin E_{PVG} (same share in the SR). Assuming a SR without the impacts of the disturbances, the resulting fuel consumption (QFC) is estimated by applying the QSP model;
- The shortfall, which therefore reflects overconsumption, is then calculated by:

$$EFG = EFC - QFC \qquad (15)$$

The estimation of a shortfall in fuel is then possible as it is shown here in the case of the day of 11 October 2019 between 8:00 a.m. and 4:00 p.m. (Figure 20). For this day, the PV electrical power delivered by the photovoltaic installation clearly indicates the effect of frequent cloud passages.
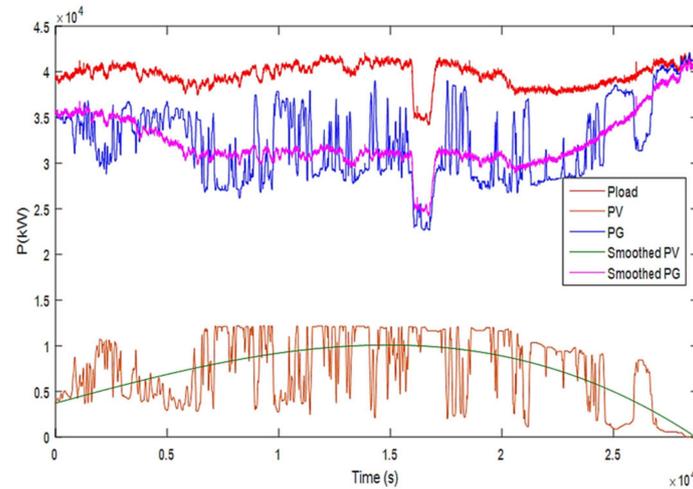

Figure 20. Illustration of the overall effect of overconsumption.

The applicable PSD model leads to the actual consumption of generators (EFC). According to the previous procedure, the "Averaged PV" (PVA) curve producing the same PVG's energy is computed. Accordingly, the operation of the groups would be with the QSP behavioral model. The idealized equivalent operation according to a quasi-static evolution provides the corresponding QFC, allowing the shortfall EFG calculation (Equation (15)).

- It is observed that the specific consumption provided by the model between 8:00 a.m. and 4:00 p.m. on 11 October 2019 is slightly higher than the value provided by the meters (0.8%). This small deviation validates the model;
- The solar production for this day of 11 October 2019 was thus estimated 58,408 kWh. Compared with actual production, the idealized smoothed production yielded 1009 kg shortfall in fuel. This method can therefore be judiciously generalized and adopted for day-to-day estimation.

3.2. Expected, Achieved and Achievable Energy Contribution of PV

A conclusive assessment of the relevance of the QSP and DSP models was proposed based on comparisons with operating data corresponding to real plant operating conditions.

With these behavioral models, performance indicators can be developed to help in selecting improvement options for the system. The aim is to evaluate the impact of PV power injection on fuel consumption.

Indicators for analyzing the operation of the Essakane PV/Diesel Hybrid Power Plant have been constructed. The real energy contribution of the solar power plant estimated the sunshine regime (quasi-static or dynamic) through operating scenarios. Seasonal changes led us to consider three reference scenarios that provide us with three basic indicators (adaptable to various viewing windows), thus, we have:

- The TWS (Thermal Without Solar) scenario: In this scenario, the SR is accomplished by the gensets alone. This makes it possible to calculate the maximum fuel oil (MF) potentially required and the corresponding specific consumption (SC);
- The MST (Mean Solar/Thermal) scenario: In this scenario, the SR is accomplished by the thermal groups and the idealized "medium" solar. It allows to evaluate the expected fuel gain (FG) by power injection at the "sun's edge" without any perturbation of the sunshine. This FG is also evaluated by simulating an "equivalent" average sunshine effect. Doing so allows to calculate the specific consumption (CS) corresponding to this expected behavior scenario;

- The DST (Disturbed Solar/Thermal) scenario: In this scenario, the SR is accomplished by the thermal groups and the so-called "disturbed" solar (DSP). It makes it possible to calculate the shortfall (EFG) by comparing the (EFC) to the simulated QFC for any observation window.

Based on these scenarios, we synthesized three performance indicators including: fuel saved (FS), energy shortfall (EFG), and specific consumption (SC). Finally, options for improving the energy efficiency of the hybrid plant are proposed.

3.2.1. Impact of PV Power Injection on the Performance of the Thermal Power Plant

In order to illustrate the impact of solar generation on the performance of the thermal plant (regardless of the sunlight profile), we considered an observation window from 4:00 a.m. to 8:00 p.m. for the day of 17 July 2020. This day is characterized by a typical load profile (evolving low frequency) and a fluctuating solar PV generation profile, as shown in Figure 21.
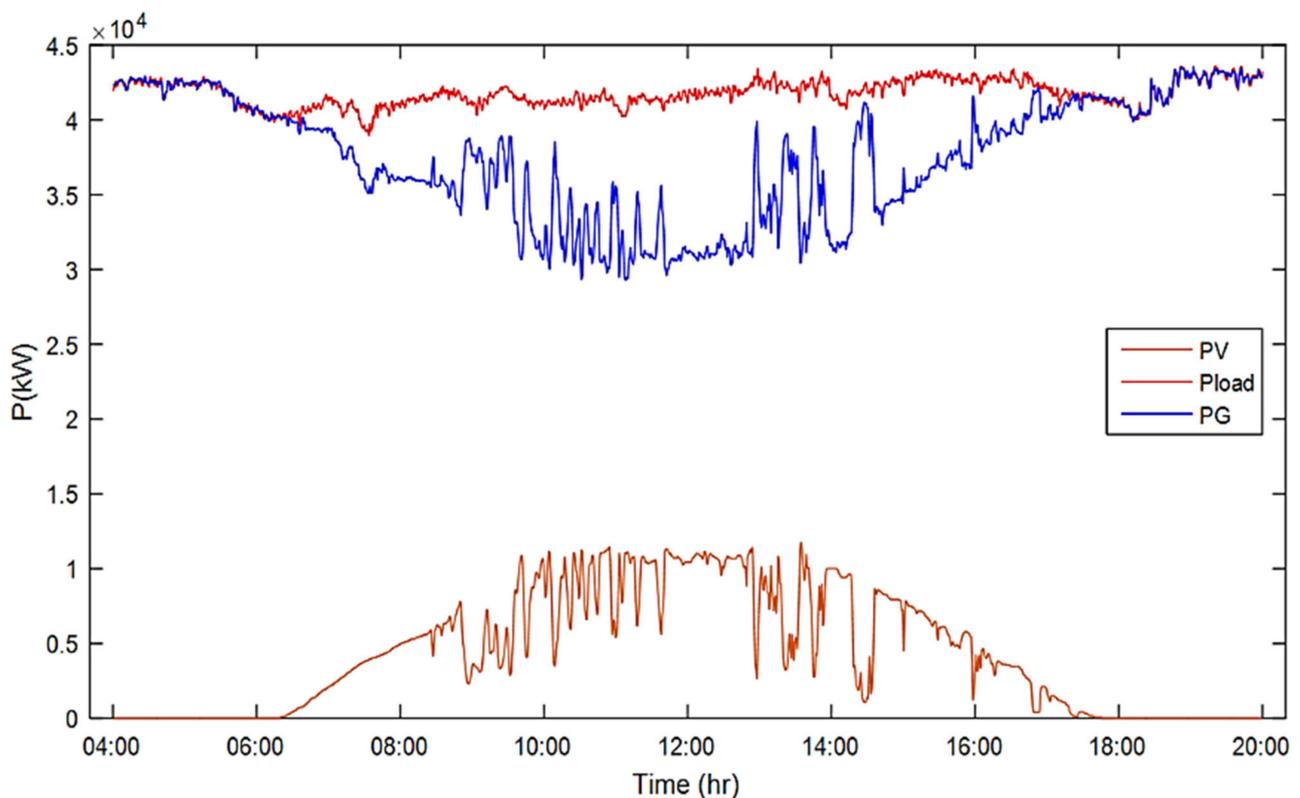

Figure 21. Observation window of the impact of solar energy (PV) and the service to be rendered (P load).

The number of groups in operation during this period is nine (plus or minus one) units related to plant operating rules. We examined the evolution of the fuel oil consumption and the specific consumption of the thermal power plant (Figure 22).
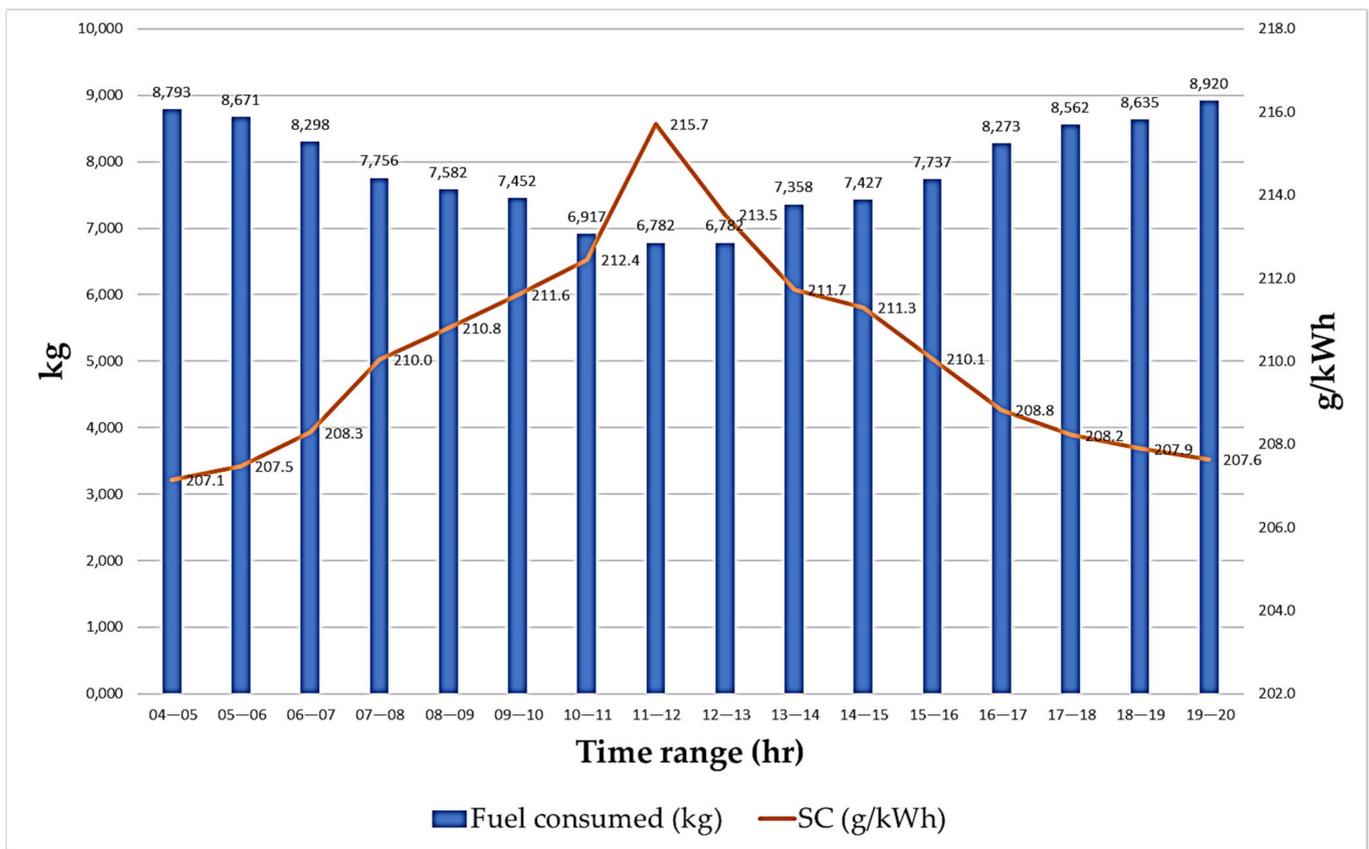
Figure 22. Fuel consumed (kg) and SC (g/kWh) of the thermal power plant (17 July 2020).

In this graph, we observe that hourly FC evolves between 8920 kg/h to 6782 kb/h opposite to sunrise. These results show a substantial increase in SC, 207 g/kWh to 216 g/kWh, signifying a degradation in the efficiency of the thermal units. Indeed, this tendency that we call "downgrading" is stepped up by a penalty of frequent disturbances.

3.2.2. Enhancement Capability Evaluation by Means of Indicators

Thus, the ESR for the TWS scenario is fulfilled, with related maximum fuel consumption without hybridization of the power plant. There is no fuel saved. The FS is the fuel saved under scenarios, actual (DST), or idealized (MST), using established models in case. It goes without saying that the effect of spinning reserve control on the number of active thermal units, if any, is included.

For example (Table 6), to evaluate the fuel gained (FS) for the day 17 July 2020 from 4:00 a.m. to 8:00 p.m., we first evaluated the FC by considering the TWS scenario. We have thus calculated 137,780 kg for an electrical energy production of 668,631 kWh, i.e., an estimated specific consumption close to 206 g/kWh. For the scenario corresponding to the real operation of the hybrid power plant, the data from the meter readings of the hybrid power plant indicate a real fuel consumption of 125,945 kg for an electrical energy production of thermal group of 600,020 kWh. The FS corresponds to 11,835 kg. The units have performed a specific consumption of 209.72 g/kWh. We have then developed the MST scenario and have calculated a consumption of 125,220 kg. Comparing the fuel consumption in the DST scenario with the fuel consumption that would occur in the MST scenario, this results in a deficit (EFG) of 725 kg.

Table 6. Summary of fuel consumption mixed scenario QSP and DSP (Day: 17 July 2020).

Day: 17 July 2020 4:00 a.m. to 8:00 p.m. Load Profile: Static PV Profile: Dynamic	Designation-Production and Consumption				Performance Indicator		
	E_{SR} (kWh)	E_{TPS} (kWh)	E_{PVG} (kWh)	FC (kg)	FS (kg)	EFG (kg)	SC (g/kWh)
TWS Scenario	668,631	668,631	0	137,780	0	NC	206
DST scenario	668,631	600,020	68,711	125,945	11,835	hident	209.72
MST Scenario	668,631	599,800	68,630	125,220	12,560	725	208.7

Based on these results, Table 6, we consider the value of fuel saved (FS), the shortfall (EFG), and the specific consumption (SC), as performance indicators for the hybrid plant. One way to optimize the operation of the hybrid power plant is to increase the value of the FS while minimizing the value of the EFG, and the value of the SC.

The study of the impact of transient regimes due to the variations of the load or of the sunshine, and those more rapid such as cloudy sky PV power injection, make us identify two major constraints to mitigate effects to trend toward the hybrid plant effectiveness enhancement:

- Fluctuation of the PV production: Indeed, for the operations impacted by frequent sunshine disturbances (cloudy passages), we have established that the consumption model is penalized by an overconsumption. Mainly due to the dynamic acceleration-deceleration regime of the internal combustion generators, it is known that an increase in pollution due to the emission of harmful gases and particles also occurs. Fouling of the combustion chamber components leads to more expensive maintenance;

- Derating of thermal units: According to the current operating strategy of the hybrid plant, the spinning reserve must remain above 80% of the active power supplied by the solar plant. As a result, more generators than necessary for the powering are kept in operation. In addition, due to the unavoidable variation in sunlight between sunrise and sunset, there is a shift in the operating points of the active generators with respect to a rated reference. This behavior induces a derating factor for the power units. The further the operating point is from the nominal point, the worse the efficiency.

In order to insure QSP behavior independent of weather induced disturbances on sunlight, we investigated the option of "Compensation of the Fluctuations Only" (CFO). In an ideal case, the fuel saved will increase and the TPS will perform better (Figure 23). The expected result is given by a previous estimation, such as in the sample case of day 17 July 2020. Fluctuation compensation and derating (CFD) management by the operating strategy constitute a second enhancement possibility. The adaptation of the operating strategy consists here in reviewing the constraint on the spinning reserve. It is set to 80% of the active power of the solar generation. In order to achieve this, the number of active generators is increased at the cost of lowering the unit efficiency. For the day 17 July 2020, the analysis of the profile of the spinning reserve shows that the hybrid plant could operate with one less unit once the fluctuation compensation mechanism is settled. The risk of crossing the limits of the spinning reserve becomes less. The loading ratio of remaining active genset units increases as well as the efficiency for the same P_{SR}.

Table 7 gives the synthetic balance from the energy view point for this second option. The balance indicates a substantial fuel saving of 1995 kg. This result shows that by addressing the derating enlargement phenomenon, the fuel saving would be more substantial.
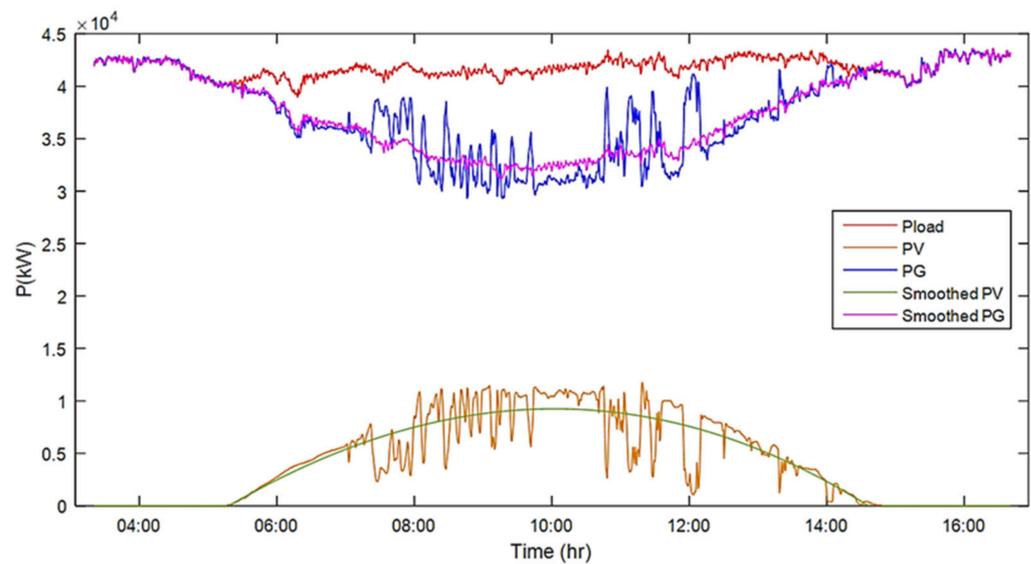
Figure 23. Ideal compensation of PV disturbances.

Table 7. CFD derating management additive benefit.

Day: 17 July 2020 from 4:00 a.m. to 8:00 p.m.	E_{SR} (kWh)	E_{TPS} (kWh)	E_{PVG} (kWh)	FC (kg)	EFG (kg)
DST scenario	668,631	600,020	68,711	125,945	1995
MST Scenario	668,631	599,800	68,630	125,220	

4. Discussion

4.1. Technical and Economic Evaluation of the Enhancement of Options

4.1.1. Selected Potential Gain Options for Consideration

As the negative impact of dynamic solar disturbances and the evolution of daily sunshine has been demonstrated, we propose to remedy this by, for example, including storage units, or by modifying the management strategy. As outcome, a new candidate architecture could be envisaged, which would consist of going forward with hybridization by adding electrochemical storage technology capable of compensating solar power fluctuations penalties. The choice of technology would be guided by the good compromise between the abilities facing energy density versus power density, as well as the sensitivity to micro charge cycles. Among the existing solutions, lithium batteries with a total calculated capacity of 6600 kWh could be suitable. However, it is necessary to ensure a payback on investment within a reasonable period in order to judge the solution to be satisfactory (fuel savings, low level of investment, and operating cost). An approach that can be used in the design and sizing of standalone PV/Diesel power plants, taking the context of the Essakane mine as a reference, has been developed. It integrates the behavioral impacts of sunshine fluctuation dynamics on site. Furthermore, the decision support approach, which is very specific to a mining site, can be adapted to other situations as long as the service to be rendered is well characterized and the sources of disturbances well identified (micro grid for instance).

A techno-economic analysis can benefit from the indicators developed above. The year 2020 has been chosen as the reference year for the analysis. The aim is to evaluate the fuel gain for the different options designed and extrapolate the results over several years. The observation of the solar radiation behavior on the site of the hybrid power plant (Figure 8) for the period of 2019 to 2020, showed that:

- A period of strong disturbances: this is the period from May to September and corresponds to the rainy season of the mine site;
- A period of moderate disturbances: this is the period from October to April, which corresponds to the dry season of the mining site.

Table 8 summarizes the results obtained in 2020.

Table 8. Comparative analysis of potential fuel gains based on design options 1 and 2 for the year 2020.

| Observation Windows | Year 2020 Fuel (LVH in 2020) = 40,700 kJ/kg | | | | | |
	TWS Scenario FC (kg)	Scenario DST (Meter Values) FC (kg)	MST Scenario (Simulated) FC (kg)	Fuel Gained FG (kg)	EFG CFO Option (kg)	EFG CFD Option (kg)
August (30 days)	5,137,400 100%	4,859,013	4,812,600	100% 314,387 6%	+15% 46,413	+28% 87,813
October (30 days)	5,891,346 100%	5,529,301	5,500,080	100% 362,045 6%	+8% 29,221	+18% 65,535
Annual extrapolation (2020)				100% 4,106,250	+10% 436,612	+22% 897,810

The economic gains assessment of the options for year 2020, are based on the following assumptions:

- The density of the fuel used is 0.970 kg/L;
- The cost of HFO is 0.75 USD/L.

These data come from the daily operating reports of the hybrid power plant.
Table 9 summarizes the potential cash savings for the year 2020.

Table 9. Potential fuel savings under CFO and CFD for the year 2020 and corresponding cash savings.

	FS (kg)	Fuel Density in kg/L	FS (L)	Fuel Cost in USD/L	Cash Saved (USD)
CFO Option	436,612	0.970	450,115	0.75	337,586
CFD Option	897,810	0.970	925,577	0.75	694,182

4.1.2. Storage Sizing

For the sizing of the batteries used to compensate the fluctuations:

- The first step is to evaluate the energy needed to be stored each day with disturbances. The residual profile, obtained by differentiating the instantaneous $PV_d(t)$ and averaged $PV_{dave}(t)$, provides storage energy evolution. A daily evolution $Estock_D(t)$ is calculated by Equation (16).

The amount of energy to be stored (ΔE_D) for D-day is then obtained by Equation (17) expressing the difference between extrema of $E_{stockD}(t)$.

$$E_{stockD}(t) = \int_D (PV_d(t) - PV_{dave}(t))dt \tag{16}$$

$$\Delta E_D = \max(E_{stockD}(t)) - \min(E_{stockD}(t)) \tag{17}$$

- The second step of the approach consists in determining the storage capacity for the "worst case" i.e., for the most restrictive day. The variability of solar radiation from one day to another, from one season to another, or from one year to another, induce following assumptions:
    1. The most restrictive days are the cloudy ones on site (in particular the July–August in chosen case);
    2. Solar radiation behaves statistically the same from one year to another on site.
- In the third step, the same time trade-off analysis among different storage technologies must be performed to make a choice according to the LCOE targeted.

Considering a conventional depth of discharge of $\delta\%$, the final capacity to select is equal to: $\frac{max(\Delta E_D)}{\delta}$.

Application to the Essakane PV/Diesel Hybrid Power Plant

Application of the method for the day of 28 August 2020 as a single detailed example.

The averaged PV power is represented in green color (Figure 24). The profile of the residual power in blue color (Figure 25) results from the difference between the actual and the averaged power. The total sunshine duration had been about $\Delta t = 11$ h.
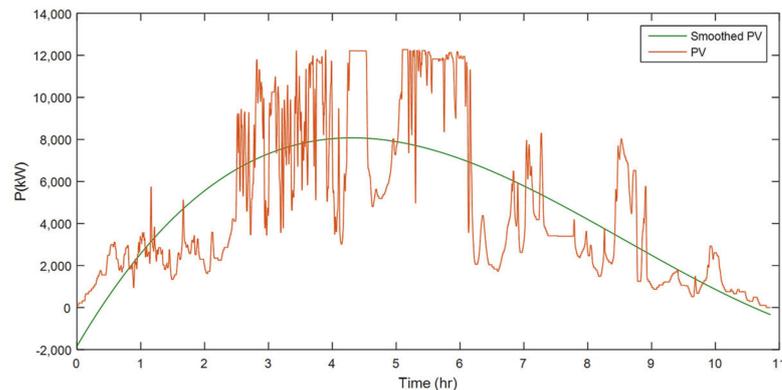

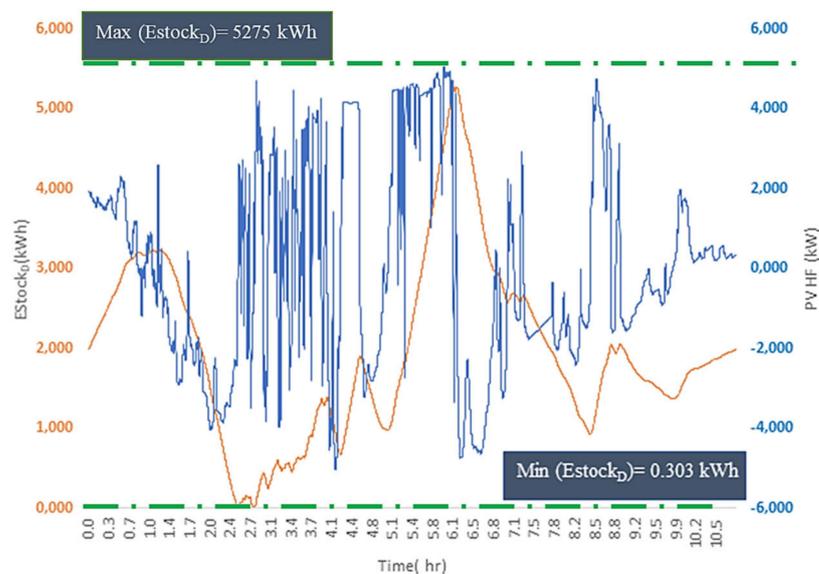**Figure 24.** Actual and averaged PV power of day 28 August 2020.

Figure 25. Evolution E_{stock} and PVHF residue profile of 28 August 2020.

Thus, an assessment of the energy to be stored was carried out for all the days of relevant months of the year. This day-to-day assessment was considered on the August representative profile, in Figure 26.
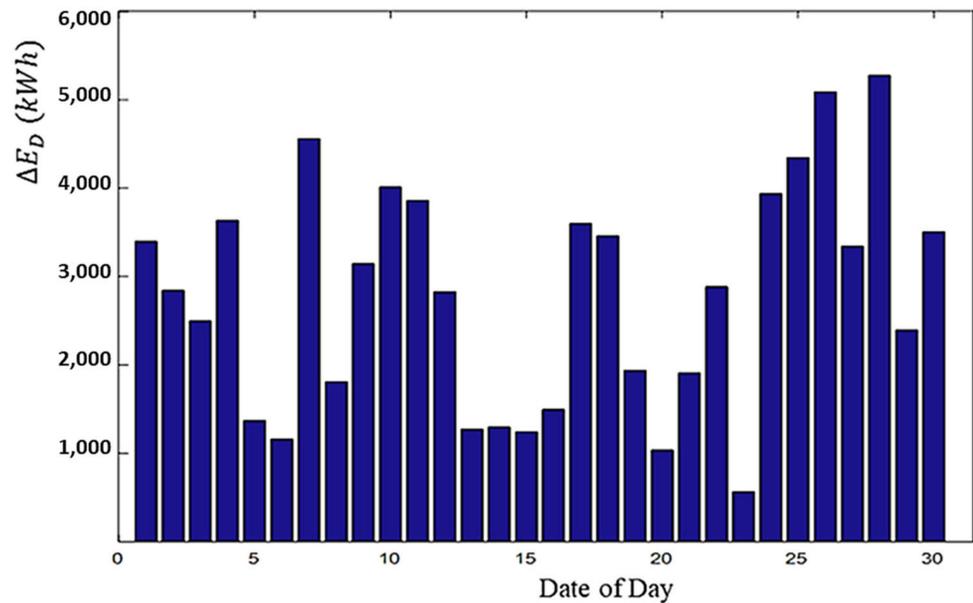

Figure 26. Evolution of the energy to be stored day-to-day for the month of August 2020.

The value of energy to be stored for this operating day of 28 August 2020 (Figure 25) have been found ΔE_D = 5275 kWh. By applying a depth of discharge of 80% it yielded 6600 kWh storage capacity.

A frequency domain analysis and a Ragone plot assisted design help to make the right choice of storage technology [12]. In the following, the lithium battery has been chosen.

4.2. Production Cost and LCOE Analysis Performed Coupled to Energy Storage

4.2.1. Production Cost and the LCOE of the Thermal Power Plant Alone

The determination of the production cost of the thermal power plant consists in a way, in determining the cost of energy over an annual horizon. While the Levelized Cost of Energy (LCOE) gives the average cost of energy over the life of the project. These indicators are given by the following expressions:

$$\text{Annual production cost} = \frac{\text{OPEX}}{E_a} \tag{18}$$

OPEX = Cost of annual fuel consumption + Cost of operations and maintenance + cost of energy purchase;

E_a = Annual energy production in kWh.

$$\text{LCOE} = \frac{\text{Lifecycle cost}}{\text{life time energy production}} \tag{19}$$

The approach to the calculation of LCOE adopted can be found in full detail in [6,31] (pp. 67–71). Life Cycle Cost represents the total system cost over the life of the system updated to year 0. It includes Initial Cost, Operating Cost and Maintenance Cost.

For the PV power plant alone, the cost of purchasing energy is zero and we considered the operating data of the thermal power plant from 2016. Table 10 gives the assumptions and results of the economic calculation.

Table 10. Assumptions for the thermal power plant alone [2,6,23,33] LCOE calculation result.

Assumptions	
Designation	**Value**
Initial cost in USD/kW (Diesel)	582
O&M cost in USD/kWh (Diesel)	0.05
Fuel cost in USD/L	0.75
HFO density in kg/L	0.970
Discount rate e	8%
Inflation rate i	2%
Project lifetime (year)	25
Fuel consumption in (L) (operating data 2016)	69,163,786
Annual electricity production (kWh) (operating data 2016)	322,543,141
Annual production cost and LCOE of the thermal power plant alone	
Annual production cost (USD/kWh)	0.211
LCOE (USD/kWh)	0.219

4.2.2. Production Cost and LCOE of the PV/Diesel Hybrid Power Plant

For the hybrid PV/Thermal power plant, the payback capability of the saved fuel by means of the energy from the solar PV plant, is computed with other relevant index. Table 11 give the assumptions and economic calculation results of the hybrid plant for the year 2020.

Table 11. Assumptions for the PV/Diesel hybrid plant [1,2,6,23,33,34] LCOE calculation result.

Assumptions	
Designation	**Value**
Initial cost in USD/kW (Diesel)	582
Initial cost in USD/kW (PV)	883
O&M cost in USD/kWh (Diesel)	0.05
O&M cost in USD/kW (PV)	40
Cost of purchasing electricity in USD/kWh	0.16507
HFO density in kg/L	0.970
Fuel cost in USD/L	0.75
Discount rate e	8%
Inflation rate i	2%
Project lifetime	25
Thermal power plant life	25
Solar power plant lifetime	25
Solar production in 2020 in kWh	23,593,388
Thermal production in 2020 in kWh	312,468,274
Fuel consumption in 2020 in Liter	67,196,785
Production cost and LCOE of the PV/Diesel hybrid plant in the current configuration	
Annual production cost in USD/kWh	0.207
LCOE in USD/kWh	0.209

We also proceeded to the profitability analysis of the implementation of a storage system for the hybrid plant. Choosing lithium batteries, the cost-benefit analysis consisted in evaluating the investment cost of the storage system based on cost per kWh and the O&M cost of such technology implementation. Tables 11 and 12 give a summary of the assumptions used for economic evaluation of the storage solution. Comparative cost of investment deduced, for the all plant, without variable costs, would be roughly 50 M$ (68% diesel plant, 27% PV plant, 5% storage unit) Assuming that the implementation of storage will improve the efficiency of the thermal units and will also generate additional fuel savings. This gain has been estimated using the proposed method at 925,577 L of potentially saved fuel for the year 2020 as example.

Table 12. Economic calculation assumptions for Lithium batteries [34] and comparative summary of LCOE of the alternatives.

Assumptions	
Designation	**Value**
Initial cost in USD/kWh (Lithium Battery)	350
O&M cost in USD/kWh (Lithium battery)	10
Lifespan (Lithium Battery)	15 years
GAIN of fuel oil in liter (In reference year 2020)	925,577
Fuel cost in USD/L	0.75
Different plant configurations	LCOE (USD/kWh)
Thermal configuration only	0.219
Current PV/Diesel configuration	0.209
PV/Diesel configuration with storage and derating management	0.205

5. Conclusions

Behavioral models with the aim of decision-making support allow us to estimate both thermal engines and photovoltaic generators' steady-state and dynamic power interaction conditions. The parameters of the models match with commercial design software ones. They have been fitted from data carried out from a multimegawatt hybrid power plant operating in a Sahelian area mine site. Season dependent disturbance effects have been more explicitly considered into long-term scenarios simulation to assess relevancy in environmental impact. As a better quantification tool, these models allow us to calculate the LCOE as the average cost per kWh of electrical energy produced by the system. This approach can be used to reevaluate the payback for a project in a specific climatic area.

Author Contributions: Conceptualization, S.M.K. and B.D.; methodology, B.D.; software, S.M.K.; validation, B.D., Y.C. and M.B.C.; formal analysis, B.D., Y.C. and M.B.C.; investigation, B.D.; data curation, S.M.K.; writing—original draft preparation, S.M.K. and B.D.; writing—review and editing, B.D.; supervision, Y.C. and B.D.; project administration, B.D.; funding acquisition, B.D. and Y.C. All authors have read and agreed to the published version of the manuscript.

Data Availability Statement: Not applicable.

Conflicts of Interest: The authors declare no conflict of interest.

Abbreviations

AC	Alternating current
B_{Nu}	Consumption of N gensets when electrical supplied is zero
B_u	Consumption of one genset when electrical supplied is zero
CFD	Compensation of Fluctuations and Derating management option
CFO	Compensation of the Fluctuations Only option
CFS	Compensation of Fluctuations by staggered storage power option
DC	Direct Current
DSM	Demand Side Management
DSP	Dynamic Solar Profile
DST	Disturbed Solar/Thermal scenario

EFC	Effective fuel consumed
EFG	Shortfall
E_{PVG}	Solar energy production (kWh)
E_{SR}	Electrical consumption (kWh)
E_{TPS}	Thermal energy production (kWh)
FC	Fuel Consumption
FC_A	Annual fuel consumed
FS	Fuel Saved appliying a given scenario
FSM	Fuel saving margin
G	Irradiance in W/m^2
$G_1 \dots G_{12}$	Nomenclature of gensets
HFC_{Nu}	Hourly fuel Consumption per N producing unit (kg/h/kW)
HFC_u	Hourly fuel Consumption per single producing unit (kg/h/kW)
HFO	Heavy Fuel Oil
MF	Maximum Fuel oil potentialy required for thermal gensets working alone
MST	Mean solar/Thermique scenario
OPEX	Operating expenses
PCC	Point of Common Coupling
PG	Thermal plant power generation in kW
PG_{Nu}	Electrical power supplied per N producing units in kW
PG_u	Electrical power supplied per producing unit in kW
P_n	Rated Power in kW
P_{SR}	Electrical demand Profile
PV	Solar Power in kW
$PV_d(t)$	Instantaneous PV Power of D day
$PV_{dave}(t)$	Instantaneous averaged PV Power of D day
PVG	Photovoltaic generator
QFC	Fuel consumed by applying QSP model
QSP	Quasi-static solar Profile
QSP-E	Equivalent of Quasi-static solar Profile
RNI	Burkina's National Interconnected Grid
SBM	Seasonal Behavioral Models
SC	Specific Consumption
SR	Service to be rendered
T_1, T_2, T_3	Transformer
TPS	Thermal Power Station
TWS	Thermal power without solar

References

1. IRENA. *Renewable Power Generation Costs 2020*; IRENA: Abu Dhabi, United Arab Emirates, 2021.
2. Blechinger, P.; Cader, C.; Bertheau, P.; Huyskens, H.; Seguin, R.; Breyer, C. Global Analysis of the Techno-Economic Potential of Renewable Energy Hybrid Systems on Small Islands. *Energy Policy* **2016**, *98*, 674–687. [CrossRef]
3. Cader, C.; Blechinger, P.; Bertheau, P. Electrification Planning with Focus on Hybrid Mini-Grids—A Comprehensive Modelling Approach for the Global South. *Energy Procedia* **2016**, *99*, 269–276. [CrossRef]
4. Moner-Girona, M.; Solano-Peralta, M.; Lazopoulou, M.; Ackom, E.K.; Vallve, X.; Szabó, S. Electrification of Sub-Saharan Africa through PV/Hybrid Mini-Grids: Reducing the Gap between Current Business Models and on-Site Experience. *Renew. Sustain. Energy Rev.* **2018**, *91*, 1148–1161. [CrossRef]
5. Bissiri, M.; Moura, P.; Figueiredo, N.C.; Pereira da Silva, P. A Geospatial Approach towards Defining Cost-Optimal Electrification Pathways in West Africa. *Energy* **2020**, *200*, 117471. [CrossRef]
6. Ouedraogo, B.I.; Kouame, S.; Azoumah, Y.; Yamegueu, D. Incentives for Rural off Grid Electrification in Burkina Faso Using LCOE. *Renew. Energy* **2015**, *78*, 573–582. [CrossRef]
7. Kadri, S.M.; Bagre, A.O.; Camara, M.B.; Dakyo, B.; Coulibaly, Y. Electrical Power Distribution Status in West Africa: Assessment and Perspective Overview. In Proceedings of the 2019 8th International Conference on Renewable Energy Research and Applications (ICRERA), Brasov, Romania, 3–6 November 2019; pp. 511–515. [CrossRef]
8. Polleux, L.; Guerassimoff, G.; Marmorat, J.-P.; Sandoval-Moreno, J.; Schuhler, T. An Overview of the Challenges of Solar Power Integration in Isolated Industrial Microgrids with Reliability Constraints. *Renew. Sustain. Energy Rev.* **2022**, *155*, 111955. [CrossRef]
9. Tankari, M.A.; Camara, M.B.; Dakyo, B.; Lefebvre, G. Use of Ultracapacitors and Batteries for Efficient Energy Management in Wind–Diesel Hybrid System. *IEEE Trans. Sustain. Energy* **2013**, *4*, 414–424. [CrossRef]

10. Ansong, M.; Mensah, L.D.; Adaramola, M.S. Techno-Economic Analysis of a Hybrid System to Power a Mine in an off-Grid Area in Ghana. *Sustain. Energy Technol. Assess.* **2017**, *23*, 48–56. [CrossRef]

11. Datta, M.; Senjyu, T.; Yona, A.; Funabashi, T.; Kim, C.-H. A Frequency-Control Approach by Photovoltaic Generator in a PV–Diesel Hybrid Power System. *IEEE Trans. Energy Convers.* **2011**, *26*, 559–571. [CrossRef]

12. Tani, A.; Camara, M.B.; Dakyo, B. Energy Management in the Decentralized Generation Systems Based on Renewable Energy—Ultracapacitors and Battery to Compensate the Wind/Load Power Fluctuations. *IEEE Trans. Ind. Appl.* **2015**, *51*, 1817–1827. [CrossRef]

13. Anoune, K.; Bouya, M.; Astito, A.; Abdellah, A.B. Sizing Methods and Optimization Techniques for PV-Wind Based Hybrid Renewable Energy System: A Review. *Renew. Sustain. Energy Rev.* **2018**, *93*, 652–673. [CrossRef]

14. Al-falahi, M.D.A.; Jayasinghe, S.D.G.; Enshaei, H. A Review on Recent Size Optimization Methodologies for Standalone Solar and Wind Hybrid Renewable Energy System. *Energy Convers. Manag.* **2017**, *143*, 252–274. [CrossRef]

15. Tazvinga, H.; Xia, X.; Zhang, J. Minimum Cost Solution of Photovoltaic–Diesel–Battery Hybrid Power Systems for Remote Consumers. *Sol. Energy* **2013**, *96*, 292–299. [CrossRef]

16. Kusakaka, K.; Phiri, S.F.; Numbi, B.P. Optimal Energy Management of a Hybrid Diesel Generator and Battery Supplying a RTG Crane with Energy Recovery Capability. *Energy Rep.* **2021**, *7*, 4769–4778. [CrossRef]

17. Tawfik, T.M.; Badr, M.A.; El-Kady, E.Y.; Abdellatif, O.E. Optimization and Energy Management of Hybrid Standalone Energy System: A Case Study. *Renew. Energy Focus* **2018**, *25*, 48–56. [CrossRef]

18. Sinha, S.; Chandel, S.S. Review of Software Tools for Hybrid Renewable Energy Systems. *Renew. Sustain. Energy Rev.* **2014**, *32*, 192–205. [CrossRef]

19. Belmili, H.; Haddadi, M.; Bacha, S.; Almi, M.F.; Bendib, B. Sizing Stand-Alone Photovoltaic–Wind Hybrid System: Techno-Economic Analysis and Optimization. *Renew. Sustain. Energy Rev.* **2014**, *30*, 821–832. [CrossRef]

20. Ammari, C.; Belatrache, D.; Touhami, B.; Makhloufi, S. Sizing, Optimization, Control and Energy Management of Hybrid Renewable Energy System—A Review. *Energy Built Environ.* **2022**, *3*, 399–411. [CrossRef]

21. Louis, L.; Polleux, L.; Sandoval-Moreno, J.; Guerassimoff, G.; Marmorat, J.-P. Impacts of Thermal Generation Flexibility on Power Quality and Lcoe of Industrial Off-Grid Power Plants. In Proceedings of the 11th International Conference on Applied Energy (ICAE2019), Västerås, Sweden, 12–15 August 2019. [CrossRef]

22. Limpitlaw, D. *Renewable Energy in the Minerals Sector: Assessing Opportunities for Africa*; No. 326, 26; South African Institute of International Affairs: Johannesburg, South Africa, 2021.

23. Reiners, N.; Bopp, G.; Wullner, J.; Yadav, R.G. *Optimal Integration of Photovoltaics in Micro-Grids That Are Dominated by Diesel Power Plants*; Technique Report IEA-PVPS T9-19:2019; IEA: Paris, France, 2019; p. 40.

24. Multon, B.; Moine, G.; Aubry, J.; Haessig, P.; Jaouen, C.; Thiaux, Y.; Ahmed, H.B. Ressources Énergétiques et Solutions Pour l'alimentation En Électricité Des Populations Isolées. In *Electrotechnique du Futur 2011*; HAL Open Science: Belfort, France, 2011; 12p.

25. Vuong, Q.D.; Kim, J.; Choi, J.-H.; Lee, J.; Lee, J.; Jeon, H.; Noh, J.-H.; Yoon, S.H.; Lee, W.-J. Study on the Variable Speed Diesel Generator and Effects on Structure Vibration Behavior in the DC Grid. *Appl. Sci.* **2021**, *11*, 12049. [CrossRef]

26. Moradi, M.H.; Eskandari, M.; Showkati, H. A Hybrid Method for Simultaneous Optimization of DG Capacity and Operational Strategy in Microgrids Utilizing Renewable Energy Resources. *Int. J. Electr. Power Energy Syst.* **2014**, *56*, 241–258. [CrossRef]

27. Hamilton, J.; Negnevitsky, M.; Wang, X. The Potential of Variable Speed Diesel Application in Increasing Renewable Energy Source Penetration. *Energy Procedia* **2019**, *160*, 558–565. [CrossRef]

28. Semshchikov, E.; Hamilton, J.; Wu, L.; Negnevitsky, M.; Wang, X.; Lyden, S. Frequency Control within High Renewable Penetration Hybrid Systems Adopting Low Load Diesel Methodologies. *Energy Procedia* **2019**, *160*, 483–490. [CrossRef]

29. Bagre, A.O. Couplage de Centrales Photovoltaïques aux Réseaux Publics Instables: Application au Réseau National du Burkina Faso. Ph.D. Thesis, Université du Havre, Le Havre, France, 2014.

30. Fathima, A.H.; Palanisamy, K. Optimization in Microgrids with Hybrid Energy Systems—A Review. *Renew. Sustain. Energy Rev.* **2015**, *45*, 431–446. [CrossRef]

31. Koucoï, G.A. Gestion d'Energie Dans les Systèmes Hybrides PV/Diesel pour Zones Isolées et Rurales: Optimisation et Expérimentation. Ph.D. Thesis, Institut International d'Ingénierie de L'Eau et de l'Environnement—2iE, Ouagadougou, Burkina Faso, 2017.

32. Abdallah, T. Structures des Convertisseurs Modulaires Associes aux Technologies de Stockage: Applications aux Domaines Résidentiels et Véhicules Électriques. Ph.D. Thesis, Université du Havre, Le Havre, France, 2013.

33. Votteler, R.G. A Mining Perspective on the Potential of Renewable Electricity Sources for Operations in South Africa: Part 2—A Multi-Criteria Decision Assessment. *J. S. Afr. Inst. Min. Metall.* **2017**, *117*, 299–312. [CrossRef]

34. Lockhart, E.; Li, X.; Booth, S.S.; Olis, D.R.; Salasovich, J.A.; Elsworth, J.; Lisell, L. *Comparative Study of Techno-Economics of Lithium-Ion and Lead-Acid Batteries in Micro-Grids in Sub-Saharan Africa*; National Renewable Energy Lab. (NREL): Golden, CO, USA, 2019.